UK Centre for Ecology & Hydrology

Littlestock Brook Natural Flood Management Pilot

Hydrological and water quality monitoring and analysis report

Authors

Trill, E., Robotham, J., Bishop, J., Old, G., Rameshwaran, P., and Gasca-Tucker, D.

Date 17/06/2022

Title	Littlestock Brook Natural Flood Management Pilot
Client	Ann Berkeley
Client reference	Wild Oxfordshire
Confidentiality, copyright and reproduction	Open access
UKCEH reference	NEC07825
UKCEH contact details	Emily Trill UK Centre for Ecology and Hydrology, Wallingford, Oxfordshire, OX10 8BB t: 01491 692335 e: emitri@ceh.ac.uk
Author	Emily Trill
Signed	
Date	17/06/2022

Executive Summary

The Natural Flood Management trial:

The Littlestock Brook Natural Flood Management (NFM) trial was a 5-year project that ran from 2016 to 2021. Key objectives were to reduce flood risk to Milton-under-Wychwood and enhance the river environment. Through partnership working the Environment Agency (EA) collaborated with Wild Oxfordshire, the Evenlode Catchment Partnership (ECP), Bruern Estate and the local community to deliver NFM measures. Through two Doctoral Training Partnership PhD studentships UKCEH has undertaken a detailed monitoring campaign to assess the effectiveness of the measures on reducing flood flows and improving water quality.

Monitoring report:

This report describes the monitoring network, observational methods, equipment adopted, the data processing and analysis undertaken.

Implementation of the Natural Flood Management trial:

The trial has been implemented over five phases between March 2017 and February 2021. In March 2017, 12 woody dams were installed in the heavily incised northern tributary channel immediately upstream of Milton-under-Wychwood. The next three phases of delivery (2018-2020) implemented interventions in the upper catchment, including soil management measures on steep clay slopes and along overland flow pathways; creating nutrient retention ponds and sediment traps in fields; constructing 15 riparian field corner bunds to store over-land run-off; and installing a further 15 in-channel, bank-full woody dams. In addition, 100 m of watercourse was de-culverted and 230 m of new watercourse was created. A Forestry Commission Woodland Grant scheme delivered 14.4 ha of new riparian woodland, which aims to improve interception of rainfall and run-off and sequester carbon over time. Phase 5 of the trial was delivered in 2020/21 and included additional retention pond creation, further riparian tree planting and 900 m of field edge nutrient trapping swales.

Monitoring established:

A detailed multi-scale monitoring network was established to measure precipitation inputs, and water quantity and quality. Observations were made at the intervention scale as well as in streams leaving the catchment. The monitoring of two sub-catchments of equal area allowed for a partial before-after control-impact (BACI) experimental set up.

In December 2016 two instream water quantity and quality monitoring stations were established in the tributary draining to the Heath. In January 2017 a similar station was established on the other tributary. Water levels were recorded and later converted to river flows, using a rating curve determined from manual flow gaugings. Water quality measurements included suspended sediment and nutrient

concentrations. Continuous suspended sediment concentrations were estimated from monitoring turbidity and calibrating it to suspended sediment, using data from water samples. Instantaneous nutrient and suspended sediment concentrations were determined from samples collected either manually or using automatic water samplers.

Two rain gauges were installed during 2019 to observe precipitation inputs.

Thirteen water level sensors were installed in bunds and ponds to enable estimates of water storage when combined with topographic survey data.

Multi-parameter sondes were installed in online ponds and at specific locations in streams to observe their water quality.

Data and their availability:

Total data coverage for the monitoring period is over 90% across all sensors.

All data (raw, and where available quality controlled and processed) will be made available on the NERC Environmental Information Data Centre.

Flow, turbidity, suspended sediment concentration and total phosphorous data for the three main stream monitoring sites are already available for the period 2017-2021 on the EIDC (https://doi.org/10.5285/9f80e349-0594-4ae1-bff3-b055638569f8).

Data analysis:

Specific analysis reported include the following:

Daily and annual rainfall

Annual river flows

Annual fluxes of suspended sediment and nutrients

Sediment and nutrient accumulation in bunds

Sediment and nutrient attenuation in online ponds

Water storage in bunds and estimated reductions in catchment outlet peak flows during selected events

Monitoring evaluation:

Data were evaluated using a number of approaches at multiple spatial scales in order to determine the effect of the NFM interventions. Isolating the effect of the NFM from natural variability was challenging purely using an experimental BACI approach, particularly as the catchment interventions were incrementally added throughout the monitored period. Intervention-scale monitoring (e.g. continuous measurements of water depth/volume within flood storage features) provided us with evidence of the effectiveness of interventions. The intervention-scale monitoring data were used to enable estimation of the effect (e.g. reduction in flood peak) downstream at the flood receptor.

Contents

Executive Summary 1
Contents 3
1 Introduction 5
1.1 Littlestock Brook 5
1.2 Purpose of the study 6
2 The Littlestock Brook Monitoring Network 9
2.1 History of Littlestock Brook Monitoring 9
2.2 Rainfall 11
2.3 Stream levels 13
2.4 Stream velocity 14
2.5 Stream flow 14
2.6 Stream water quality 15
2.6.1 Continuous turbidity 15
2.6.2 Instantaneous Sediment and Nutrient Concentrations 17
2.6.3 Continuous Suspended Sediment Concentration and Total Phosphorous 17
2.6.4 Multi-parameter water quality sondes 18
2.7 FSA water levels and volumes 18
2.8 Pond water quality and nutrient attenuation 20
2.9 Pond sediment and associated nutrient accumulation 22
2.10 Bund sediment accumulation 23
3 Data Coverage 26
3.1 Flow 28
3.2 Suspended Sediment Concentration 28
3.3 Rainfall 28
3.4 Atmospheric Pressure 28
3.5 FSA water levels 29
4 Analysis 30
4.1 Rainfall 30
4.2 Annual stream discharge 31
4.3 Annual fluxes of suspended sediment and nutrients 34
4.4 Sediment and nutrient accumulation in FSAs 37
4.5 Sediment and nutrient attenuation in online ponds 42
4.6 Water storage in FSAs during storm events and estimated reductions in catchment outlet flows 49
5 Monitoring Evaluation 56
6 Concluding Remarks 57

7 Acknowledgements 58
8 References 59
9 Appendices 60
9.1 Appendix 1 – Rating curves 60

1 Introduction

1.1 Littlestock Brook

The Littlestock Brook is a 16.3 km^2 sub-catchment of the River Evenlode catchment (430 km^2); located in the upper reaches of the Thames basin in West Oxfordshire, United Kingdom (Figure 1). The Evenlode catchment lithology is dominated by the Great Oolite Group, consisting of mudstone and fine-grained limestone. The Littlestock Brook sub-catchment on the west of the Evenlode is mostly underlain by the Lias Group; consisting of clays, mudstones and limestones (Robotham et al., 2021).

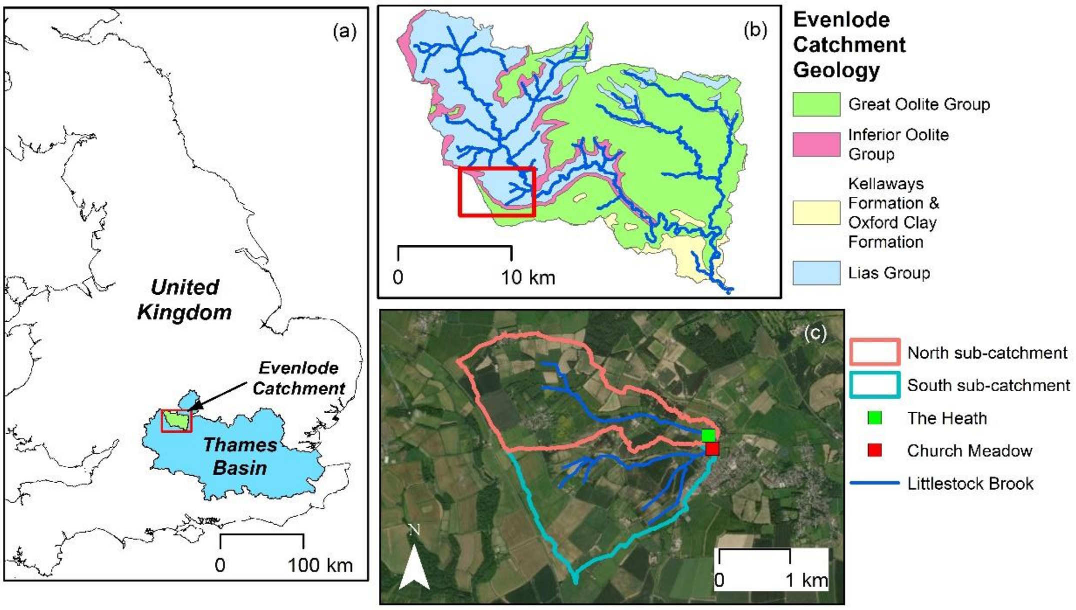

Figure 1: Locations of (a) the Evenlode catchment (green) within the Thames basin (blue); (b) the downstream catchment (outlined in red) within the Evenlode catchment and its geology; (c) the north and south sub-catchments with sub-catchment outlets marked. Adapted from Robotham et al. (2021).

The NFM trial in the Littlestock brook sub-catchment has been implemented and intensely monitored upstream of the Milton-under-Wychwood flood receptor between 2016 and 2022. Milton-under-Wychwood is at the confluence site of two tributaries draining the upstream study area that is comprised of two predominantly rural sub-catchments, each 3.4 km^2 and referred to as North and South in this report. The North sub-catchment consists mainly of arable land and permanent improved grassland used for grazing cattle and sheep, while the South sub-catchment is largely arable (Table 1).

Table 1: Land use of study site sub-catchments (% coverage), extracted from UKCEH Land Cover Map 2015.

North		South	
Broadleaved woodland	1.55	Broadleaved woodland	0
Arable and horticulture	60.59	Arable and horticulture	76.25
Improved grassland	34.66	Improved grassland	16.61
Calcareous grassland	0.66	Calcareous grassland	5.51
Suburban	2.54	Suburban	1.62

The elevation of the study area ranges from 103 m to 202 m, with an average slope of 6.4 % (Robotham et al., 2021). The area receives an average annual rainfall of 809.6 mm and experiences an average annual minimum and maximum temperature of 5.9 °C and 13.4 °C respectively (Met Office, 2022). Both sub-catchments have a low baseflow component of total stream flow, but the contribution of groundwater to river flow is greater in the south catchment. This is indicated by a higher base flow index of 0.75 relative to 0.33 in the North sub-catchment (Table 2). The Richard-Baker flashiness index indicates how quickly a stream increases and decreases during storm events, using changes in daily flows relative to average annual flows. The North sub-catchment has a higher flashiness index of 0.40 relative to the south sub-catchment index of 0.16, indicating that the short-term response to run-off events is faster in the North sub-catchment.

Table 2. Catchment and flow properties over the period January 2017 – April 2022 (Adapted from Robotham et al. 2022 (manuscript in preparation))

Catchment property		Sub-catchment North	Sub-catchment South
Flow (L s^{-1})	Q_{mean}	32.5	60.7
	Q_{50}	8.6	53.0
	Q_{10}	93.3	111.9
	Q_{1}	248.0	214.4
BFI (base flow index)		0.33	0.75
RBI (Richard Baker flashiness index)		0.41	0.16
Bedrock geology (%)	Limestone	30.0	45.0
	Mudstone	49.6	38.8
	Siltstone & mudstone (interbedded)	20.4	16.2
Average slope (%)		6.9	5.8

1.2 Purpose of the study

The Evenlode catchment has few significant settlements, with the rest of the catchment's population largely dispersed into many small towns and villages. Several of these settlements are in the upper and middle Evenlode and are prone to flooding, including the Wychwoods (Milton, Shipton and Ascott) (Old et al., 2019). Four properties flooded in 1990 and 1998, and 318 properties suffered fluvial flooding in

July 2007. After the 2007 flooding, property level flood mitigation measures and modifications to a flood storage area (FSA) were installed to reduce the flood risk from the Littlestock Brook in Milton-under-Wychwood.

As there are a relatively small number of properties vulnerable to flooding in the Littlestock Brook sub-catchment, an engineered flood mitigation scheme could not be justified on a cost-benefit basis. As the community remained vulnerable to flooding after 2007, the Environment Agency (EA) collaborated with Wild Oxfordshire, the Evenlode Catchment Partnership (ECP), Bruern Estate and the local community to trial Natural Flood Management (NFM) measures. The trial was implemented by establishing an integrated catchment partnership approach with a working group including these key organisations, local communities and landowners to develop cost-effective, sustainable NFM solutions.

Phase 1 of NFM measure implementation began in March 2017, with installation of 12 woody dams in the heavily incised northern tributary channel immediately upstream of Milton-under-Wychwood, to reduce the transport of coarse bed material restricting flow conveyance (Table 3). The next three phases of delivery (2018-2020) implemented interventions in the upper catchment, including soil management measures on steep clay slopes and along overland flow pathways; creating nutrient retention ponds and sediment traps in fields; constructing 15 riparian field corner bunds to store over-land run-off; and installing a further 15 in-channel, bank-full woody dams. In addition, 100 m of watercourse was de-culverted and 230 m of new watercourse was created. A Forestry Commission Woodland Grant scheme delivered 14.4 ha of new riparian woodland, which aims to improve interception of rainfall and run-off and sequester carbon over time.

Figure 2: (Left) Woody dam upstream of (P9, Figure 3) in the South sub-catchment; (Middle) On-line pond and wider tree planting (OLP10) in the South sub-catchment; (Right) Corner bund and flood storage area (P5) in the South sub-catchment, surrounded by tree planting.

Phase 5 of the trial was delivered in 2020/21 and included additional retention pond creation, further riparian tree planting and 900m of field edge nutrient trapping swales.

The primary NFM measure was the construction of field corner flood storage bunds. The leaky woody dams divert flood flows into the scrapes and field corner flood storage areas (FSA), which then intercept overland run-off pathways and temporarily store high flows from the brook. These NFM measures provide an approximate total of 30,000 m^3 of temporary storage across the whole NFM trial area. The FSAs included within the scope of this study, in the two study sub-catchments upstream of Milton-under-Wychwood, are shown in Figure 1.

Table 3: Timeline of the phased installation of NFM interventions and the potential cumulative storage volumes (m3) they added to the South and North sub-catchments. NB: Phase 1 interventions were not part of the official NFM scheme delivery. Adapted from Robotham et al., 2022. NB. An additional tributary containing further FSAs and additional storage volume is not included within this report.

Phase	Implementation	South sub-catchment		North sub-catchment	
		Interventions	Cumulative storage (m^3)	Interventions	Cumulative storage (m^3)
1	March 2017	None	0	Woody check dams (for bedload transport control)	0
2	February 2018	Leaky woody dams; field corner bunds and offline storage areas (P4, P5, P6, P7, P8, P9, OLP10); woodland planting; on-line ponds	11500	Woodland planting, offline storage area	140
3	February 2019	Field corner bunds and offline storage areas (OLP1, P2, P3); on-line ponds	14700	Field corner bund and offline storage area (P11, OLP11); leaky woody dam and swale; on-line pond	2020
4	Sept/Oct 2020	None	14700	Field corner bunds and offline storage areas (P12, P13)	8420
5	Winter 2020/21	Sediment/nutrient traps	14700	Sediment/nutrient traps and ponds	8420

The Littlestock Brook trial has been modelled by HR Wallingford using a full 2-dimensional InfoWorks ICM hydrodynamic model of the river channels and floodplains. HR Wallingford modelled the baseline before NFM measures were implemented, the effects of NFM measures on flooding up to Phase 3 of NFM measure implementation, potential additional NFM measures and bund failure studies of the FSAs.

The purpose of this study was to collect data to understand the functioning of the measures enabling calibration and validation of the modelling.

2 The Littlestock Brook Monitoring Network

2.1 History of Littlestock Brook Monitoring

The Evenlode has been monitored at Cassington Mill by the EA since 1970, with daily and peak flow data available from the UK National River Flow Archive. The same site has been monitored for water quality by UKCEH since 2009 (Bowes et al., 2018).

Prior to the NFM trial implementation three monitoring stations were installed by UKCEH upstream of Milton-under-Wychwood, in the winter of 2016/2017. These stations provide a continuous time-series of water level and turbidity at the locations marked in Figure 3 as ‘Upstream The Heath’, ‘The Heath’ and ‘Church Meadow’ (UTH, TH and CM respectively).

In 2018 the ECP organised a ‘hydro-hack’ event along with members of Oxford University, Atkins Consultancy, South East Rivers Trust to install water level sensors at several FSA and in-stream Phase 1 intervention sites.

In autumn 2018 two UKCEH PhD students started NFM research projects and further monitoring was implemented. This included 2 tipping bucket rain gauges; a storage rain gauge; 3 flow gauging sites; 6 automatic water samplers; 2 multi-parameter water quality sondes. The position of instrumentation is shown relative to NFM features in Figure 3. Further sediment and nutrient retention monitoring was implemented for FSAs constructed in the 2019 phase of NFM installation. Regular water quality spot sampling also started in March 2019, alongside wet-weather sampling campaigns during storm events.

After March 2021 the monitoring network was reduced to water level and rain gauge sensors. These data are available up to March 2022, when the monitoring project was completed.

The comprehensive hydrometric and water quality monitoring network focused on the south catchment, where nine Flood Storage Areas (FSAs) were monitored (Table 3; Figure 1). Three FSAs in the northern catchment were also monitored.

Discharge was estimated just upstream of the Milton-under-Wychwood confluence of both tributaries, using a stage-discharge rating curve and repeat observations of water level (corrected to datum). Rainfall was monitored using two tipping bucket rain gauges, near The Heath monitoring site at the outlet of the North sub-catchment and upstream in the Tears of Bruern in south catchment. A single storage gauge was co-located at the Tears of Bruern site and nearby Met Office Little Rissington rainfall data were available at grid reference 51.86, -1.692 (~3km from the Tears of Bruern gauges). Stream water level was monitored at eight locations across the catchment, in addition to the sites where discharge was monitored.

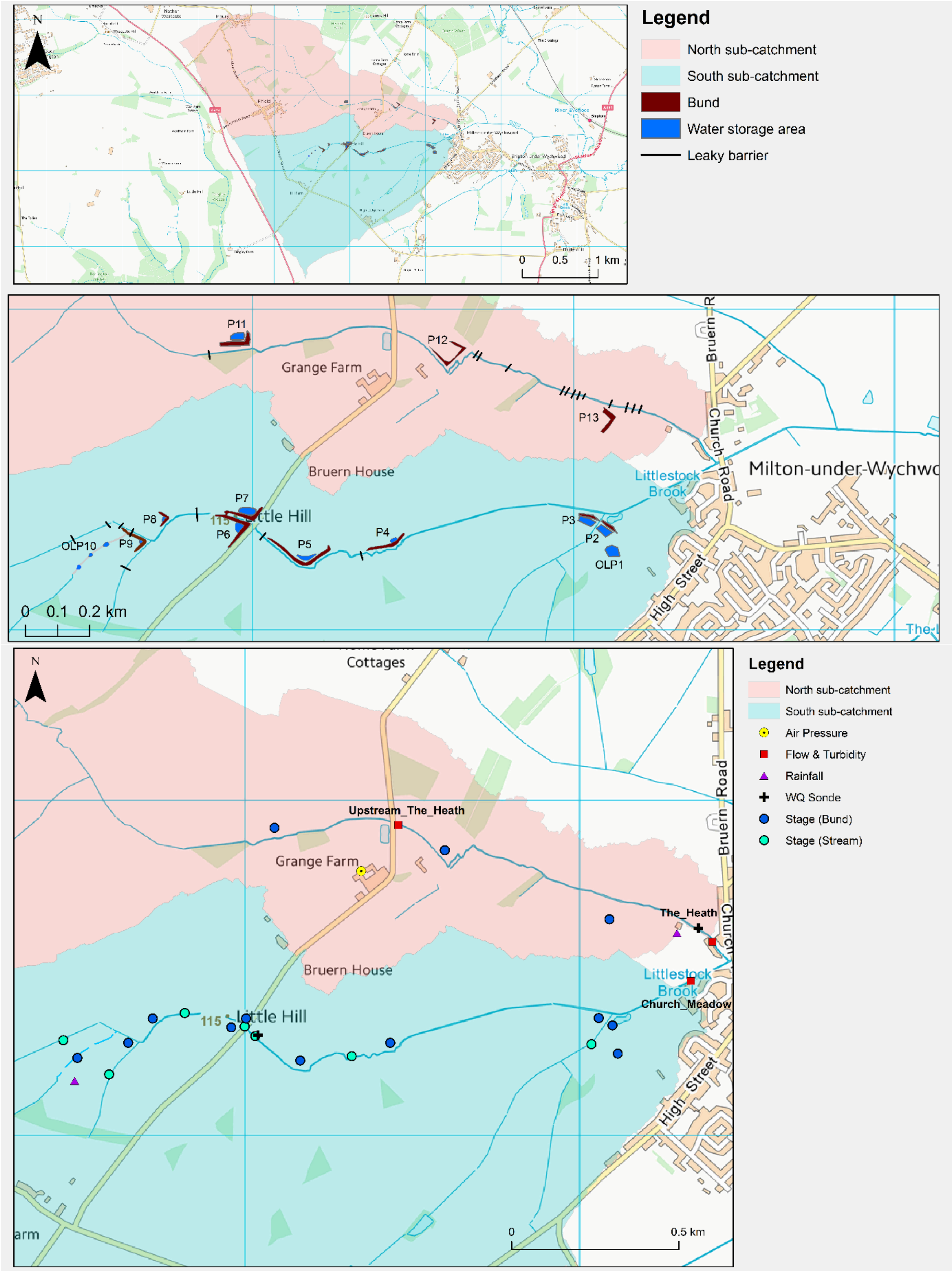

Figure 3: (Top) Overview of NFM features in the North and South sub-catchments; (middle) NFM features of the Littlestock Brook NFM Trial; (bottom) Hydrometric monitoring of the Littlestock brook. NB: OLP1 is also referred to as P1 and P1_OLP in different report sections, to keep consistent with linked publications. OLP10 includes the upstream (US) and downstream (DS) ponds referred to in water quality analysis sections and is also referred to as P10 and P10_OLP. P0_OLP is not shown on the map as it was not surveyed, did not provide additional storage potential and did not have a level sensor installed. P0_OLP is located ~100m upstream of P2 and P3.

Water quality monitoring was set up as part of the wider hydrometric monitoring network to investigate the wider benefits of the NFM scheme. Turbidity sensors were co-located at the stream discharge monitoring sites in 2016, providing detailed time-series data on sediment dynamics downstream of NFM interventions. Automatic water samplers and spot samples have been used to capture water quality dynamics during storm events at these sites, through the determination of suspended sediment and nutrient concentrations. Water quality sondes have also monitored a suite of parameters (temperature, ammonium, dissolved oxygen, pH, and conductivity) at the Heath and downstream of P6-P9 and OLP10 (Figure 3). Sediment and nutrient retention were monitored within the NFM ponds and FSAs using a combination of siltation traps, automatic water samplers, sediment coring and manual surveying.

Table 4: Hydrometric and water quality monitoring in the Littlestock Brook.

Monitored parameter	Number of sites	Monitoring interval	Instrument
Rainfall	2	2 minute	Casella Tipping Bucket Rain Gauge
Flow gaugings	2	Spot gaugings	Valeport Electromagnetic Current Meter
In-stream water level	8	5 minute	Level Troll 500/100 Data Logger
Flood storage area water level (enabling volume estimation)	11	5 minute	Rugged Level Troll 100 Data Logger
Turbidity (enabling sediment concentration estimation)	3	5 minute	FTS Digital Turbidity Sensor-12
Water quality (continuous using multi parameter sondes)	3	1 hour	EXO2 YSI sonde electrical conductivity
Water quality (regular manual spot sampling)	6	Spot samples	US DH-48 isokinetic manual sampler
Storm water quality (using automatic water samplers)	7	Spot samples	Sigma SD900 portable sampler
Sediment accumulation in online ponds (multiple siltation traps deployed at each site)	3	Spot samples	Purpose-built siltation traps (made by UKCEH)
Sediment accumulation in flood storage areas (sediment coring)	14	Spot samples	Purpose-built sediment corer (made by UKCEH)
Event response of flood storage area and leaky barrier (using time-lapse cameras)	2	1 hour	MCE-RPS-C 4G/3G Complete Camera Pillar System

2.2 Rainfall

In February 2019, a tipping bucket rain gauge (Casella; Sycamore, IL, USA) was installed in the Tears of Bruern to measure rainfall at 2-minute intervals up to March 2022. It was installed in a clearing adjacent to the upstream on-line ponds in the south sub-catchment (Figure 3), free of obstructions and cleared of surface vegetation (Figure 4). The gauge was levelled and secured. Prior to installation the rain gauge was calibrated in the lab by levelling the tipping bucket mechanism, measuring the diameter of the collecting funnel to the nearest 0.1 cm and then calculating the volume of water ($V1t$) required for the bucket to tip using:

$$V = pir^2 * resolution$$

Once $V1t$ was known water was slowly dripped into each bucket alternately using a bulb pipette, noting the volume of water required for each tip. After five repetitions, the gauge screws were adjusted and then a further five repetitions completed. This process was repeated until the volume of water required per tip matches $V1t$.

After this a burette was used to drip water (volume sufficient to produce at least 30 tips) through the rain gauge with the collector funnel attached. The expected number of tips was then compared to the recorded number of tips. If these were within 5% of each other, the rain gauge was accepted for use using the standard calibration. If the difference exceeded 5%, a new calibration would be set based on the relationship between expected and actual number of tips.

The gauge was calibrated *in-situ* at least every 6 months by repeating the last step above. Any artificial tips were removed in data processing, these were cross-checked with alternative rainfall sources to verify accuracy.

A storage rain gauge was co-located to aid quality control of the tipping bucket gauge (Figure 4). During site visits, stored rainwater was emptied into a graduated cylinder and the volume checked against the tipping bucket rainfall total for the same period to ensure measurements were within a 5% tolerance range.

Additional rainfall data are available from the Little Rissington Met Office station (grid reference 51.86, -1.692 (~3km from the 'Tears of Bruern' gauges)). There is also a privately run weather station in the nearby village of Shipton-under-Wychwood. These data were in good agreement with the Littlestock Brook rain gauge and allowed rainfall data gaps to be filled using these alternative sources (Robotham et al., 2021).

Figure 4: Tears of Bruern Casella tipping bucket rain gauge (left, white) and storage rain gauge (right, brass).

2.3 Stream levels

Water level was measured and logged at 5-minute intervals at stream sites marked in Figure 3 using a Level TROLL 100 Data Logger (pressure sensor) submerged in a plastic stilling well to minimise data noise from water turbulence (Figure 5). A barometric pressure correction was applied using equation:

$$WaterLevel = 1000 \times \frac{100 \times (TotalPressure - AtmosphericPressure)}{10^3 \times 9.81}$$

where water level is in millimetres and pressure in millibar. Quality controlled atmospheric pressure data were collected using a Rugged Level TROLL 100 sensor in a barn at Grange Farm (location marked on map as “air pressure”). Missing or suspect atmospheric pressure data were infilled or corrected using either a back-up barometric Level TROLL 100 located at the Heath or from the Met Office Little Rissington data.

Stream sites had stage boards mounted on wooden posts and surveyed to an accuracy of 1 cm using Real-time Kinematic Global Navigation Satellite System (RTK-GNSS) equipment, to enable conversion of water levels into meters above sea level (mASL). Stage board readings were taken during regular site visits and flow gaugings, and served as fixed points throughout the monitoring period. Raw water sensor water level data were corrected to stream stage using a linear regression developed between sensor values and observed stage board readings for each monitoring site. After this correction data were quality controlled for outliers and spikes.

Figure 5: Example site set up at The Heath (TH). Showing the stage board surveyed at the right of the photo, the black stilling well mounted to the wooden board and housing the TROLL pressure sensor, and the DTS-12 turbidity sensor to the left of the stilling well.

At the 3 stream monitoring sites (TH, UTH, CM), water level was measured using Vented Level TROLL 500s. These sensors did not need to be corrected for atmospheric pressure. Otherwise the level data from these sensors was processed and quality controlled in the same way as the Rugged sensors, with site specific sensor-stage board linear regression corrections and suspect data removal.

All TROLL sensors were supplied with a factory calibration and checked for clock drift at each site visit.

Additional 15-minute water level data at TH are telemetered by the EA and are publically available at https://www.gaugemap.co.uk/#!Map/Summary/17680/13431.

2.4 Stream velocity

The mean channel velocity of 0.46 m s^{-1} was estimated using a salt dilution time-of-travel experiment, using an EXO1 YSI sonde electrical conductivity (EC) sensor to measure instream specific conductivity at a 1-second resolution (Hongve, 1987). Small injections (<50 g) of table salt (Sodium Chloride) were made during a storm event at the road bridge downstream of P6 and P7 in the South sub-catchment. Two EC sensors were located at the injection site and at the downstream catchment outlet monitoring site Church Meadow. The salt time-of-travel between ECs was used to estimate the mean channel velocity. It was assumed that the velocity was constant along the watercourse of approximately 1460 m.

2.5 Stream flow

Streamflow is available at 5-minute intervals at the 3 in-stream monitoring sites (TH, UTH, CM). Discharge was estimated under low flows using a conductivity sensor (EXO1, YSI; Yellow Springs, OH, USA) and the salt dilution method as detailed in Section 2.4. Discharge was primarily estimated in higher flows using an Electromagnetic Current Meter ((ECM) Valeport; Totnes, UK) and the velocity-area method. For this, cross-sectional area was calculated by measuring water depths across the channel at regular intervals using a metre rule. At each point, flow velocity was then measured with an ECM, enabling the instantaneous discharge to be calculated using the below equation (Herschy,1993);

$$q_{5+6} = \frac{\overline{v}_5+\overline{v}_6}{2}\frac{d_5+d_6}{2}(b| \quad |6-b_5)$$

where q_{5+6} = discharge through segment 5-6;
$\overline{v}_5$, $\overline{v}_6$ = mean velocities in verticals 5 and 6
d_5, d_6= depth of flow at verticals 5 and 6;
b_5, b_6= distance from initial point on the bank to verticals 5 and 6.

The total discharge was calculated as the sum of the discharge in all segments and assumes that the velocity at each bank is zero.

Rating curves were developed for each stream monitoring site, enabling discharge estimates to be calculated from the power law relationship between observed stage and discharge. Rating curves were computed using the 'nls' package in R, with lower and upper 95% confidence intervals calculated following the method used by

Dalgaard (2004). The equations for each relationship are given in Table 5, with plots of each rating curve up to the maximum recorded stage included in Appendix 1 – Rating curves, with 95 % confidence intervals shown as red dashed lines.

To accurately estimate low flows at The Heath site, ratings were constructed for both low and high flows. Plotting separate ratings for low and high flows significantly improves estimates of baseflow discharge. Discharges calculated using the low flow relationship are much closer to the gauged values observed during baseflow gaugings. The low flow rating used only the low flow gauging measurements, which did not fit the full rating relationship. A curve with only high flow gaugings was used to estimate high flows. Rating curves were plotted using discharge (Q) measurements made at the Heath Site and non-linear least squares regressions were fitted.

Due to limited gauging measurements for UTH, the rating curve is only suitable for estimating discharge up to ~330 L s^{-1} and should not be used beyond this threshold (Robotham et al., 2022).

Table 5: Rating curve equations and confidence intervals used for discharge estimation at each monitoring site under different flow conditions. Flow units are L s^{-1}, and stage units are m.

Site Name	Flow Condition	Rating	Rating Curve Equation	n	Observed flow range
The Heath (TH)	Low	Estimate	$710377415.957 \times (Stage + 0.01)^{8.277}$	5	3.08 – 43.44
		Lower 95% CI	$796296879.462 \times (Stage + 0.01)^{8.350}$		
		Upper 95% CI	$636718094.631 \times (Stage + 0.01)^{8.207}$		
The Heath (TH)	High	Estimate	$6849.014 \times (Stage + 0.01)^{2.362}$	11	78.99 – 946.23
		Lower 95% CI	$4397.425 \times (Stage + 0.01)^{2.158}$		
		Upper 95% CI	$9599.230 \times (Stage + 0.01)^{2.509}$		
Upstream The Heath (UTH)	Low & high (<330 L s^{-1})	Estimate	$3914.873 \times (Stage)^{3.567}$	5	2.87 – 329.59
		Lower 95% CI	$4415.422 \times (Stage)^{3.790}$		
		Upper 95% CI	$3539.962 \times (Stage)^{3.373}$		
Church Meadow (CM)	Low & high	Estimate	$1417.271 \times (Stage - 0.013)^{1.167}$	15	4.47 – 668.35
		Lower 95% CI	$1341.966 \times (Stage - 0.013)^{1.169}$		
		Upper 95% CI	$1492.510 \times (Stage - 0.013)^{1.165}$		

2.6 Stream water quality

2.6.1 Continuous turbidity

Turbidity data were measured at 5-minute intervals using a DTS-12 (Digital Turbidity Sensor, Forest Technology Systems Ltd.) located in-stream and logged to a CR1000 datalogger at the three monitoring sites (TH, UTH, CM; Figure 5) between winter 2016/2017 to March 2021. In June 2017 an EXO2 optical turbidity sensor was also installed at TH. The EXO2 sonde was set to take hourly samples with a pumped system. The pumped system allowed measurements to be taken during low flows, when the DTS-12 sensor was above the water level. The pumped sample is taken into the system through a strainer in order to prevent large particles from the streambed or suspended organic debris (e.g. leaf litter) being sampled. This improved the reliability of the sensor, particularly during high flow events where the DTS-12 sensor can become obscured by debris (Robotham et al. 2021).

Turbidity values from the DTS-12 sensor were measured in NTU (Nephelometric Turbidity Unit) at a resolution of 0.01 NTU and accuracy of ±2% of reading + 0.2 NTU (0-399 NTU) and ±4% of reading (400-1600 NTU). Each turbidity measurement consists of 100 instantaneous samples from which summary statistics are computed. The median turbidity value is used as opposed to the sample mean, to minimise the risk of erroneous extreme samples biasing the value. Turbidity values from the EXO2 sensor were measured in NTU at a resolution of 0.01 NTU and accuracy of ±2% (Robotham et al. 2022).

Turbidity sensors were replaced approximately twice a year so that the sensors could be returned to the lab for calibration. Raw turbidity measurements were calibrated using linear equations specific to each DTS-12 sensor for that specific deployment period. The equations were determined by calibrating the DTS-12 sensors against polymer bead solutions covering a range of concentrations. These solutions were evaluated during each calibration exercise against a certified known 1000NTU standard using an Analite turbidity probe. This ensured solutions were of a known turbidity and any changes in probe output were due to changes in the probes and not the solutions. Calibrations took place before and after each turbidity sensor deployment, allowing any sensor drift to be monitored. As no significant drift was observed, the mean of the pre/post calibration values was used for that deployment period. The pre/post calibration values determined the minimum and maximum turbidity values used as estimated uncertainty bounds, to account for error attributed to minor sensor drift within the expected range of the instrument for the deployment period.

Turbidity data were quality controlled using a set of simple rules to remove erroneous measurements, caused by things such as sensor errors or stream debris getting caught on the optical face of the sensor. The rules are as follows:

- Raw values had to be > 0 NTU. Negative and 0 values were removed.
- Raw values had to be < 1600 NTU. Values above the detection range of the sensor were removed.
- Raw values recorded during prolonged periods of sensor failure were removed, where validated *in-situ*.
- Erroneous spikes in the time-series were removed. Spikes were identified using a formula stating that the turbidity value at a given timestep should be less than 3 times the mean average of the turbidity values for the timesteps immediately before and after.
- Erroneous drops in the time-series were removed. Drops were identified using a formula stating that the turbidity value at a given timestep should be greater than the mean average of the turbidity values for the timesteps immediately before and after divided by 3.
- Gaps in the time-series were linearly interpolated where the gap was less than 12 hours (outside of storm events). This was done using the function ‘fillMissing’ from the ‘baytrends’ package in R. During storm events, only gaps created by individual data ‘spikes’ were filled due to rapid changes in turbidity in response to rainfall.
- Gaps larger than 12 hours were left in the time-series.

There are periods where the stream water level was very low and exposed the turbidity sensor to the air, giving false turbidity readings close to zero. These values were identified and removed from the dataset where possible, but some may remain. Due to this issue there are large gaps in the turbidity data at TH early in the time-series. The installation of the EXO2 turbidity sensor at this site helped reduce this data loss.

2.6.2 Instantaneous Sediment and Nutrient Concentrations

To monitor stream water quality, samples were collected using a US DH-48 isokinetic manual sampler on a rod at regular (~monthly) visits to the 3 stream sites between 2016 and 2018. After 2018, automatic samplers (Sigma SD900, Hach; Loveland, CO, USA) were deployed at each monitoring site. These were programmed to trigger at a high water level indicative of a storm event, through pressure sensor data read by the CR1000 logger. Samples were processed for suspended sediment concentration (SSC) and volatile solids concentration (VSC) (as a proxy for organic matter) in the same way as described for the on-line pond samples in Section 2.8.

2.6.3 Continuous Suspended Sediment Concentration and Total Phosphorous

Calculation of the SSC time-series used simple linear regressions using turbidity to predict concentrations from spot water samples (Section 2.6.2) taken at the same time as the turbidity measurement. Turbidity from the in-stream sensor was calibrated against SSC and Total Phosphorus (TP) samples taken under a range of flows to give estimated time-series of SSC and TP. The regressions and the upper and lower 95% confidence intervals for each monitoring site are listed in Table 6. SSC was used as the predictor in regressions to calculate TP (Table 7).

Table 6: Regressions, confidence intervals, and summary statistics for the conversion of turbidity to SSC. All regressions were statistically significant at the p<0.001 level.

Site Name	Regression line	Lower 95% CI	Upper 95% CI	n	R^2
The Heath	SSC=1.5358×$Turbidity$	0.9354×SSC	1.0646×SSC	70	0.93
Upstream The Heath	EXO SSC=2.00248×EXO $Turbidity$	0.9482× EXO SSC	1.0518×SSC	100	0.94
Church Meadow	SSC=0.84206×$Turbidity$+4.03079	0.969×SSC	1.031×SSC	94	0.99
The Heath	SSC=1.00701×$Turbidity$	0.9806×SSC	1.019×SSC	95	0.99

Table 7: Regressions and summary statistics for the estimation of TP from SSC. All regressions were significant at the p<0.001 level.

Site Name	Regression line	n	R^2
The Heath	TP=0.0019×SSC+0.14	111	0.94
Upstream The Heath	TP=0.0018×SSC+0.15	47	0.94
Church Meadow	TP=0.0019×SSC+0.035	359	0.79

Fluxes of total suspended sediment, silt and clay, and TP were also calculated at the Downstream Catchment Outlet site, using discharge, SSC and TP data at 5-minute intervals. Fluxes were calculated by integrating the SSC/TP instantaneous load time-series for the monitoring period. Suspended sediment particle size distributions were sampled during two high flow and SSC events and measured using laser diffraction particle size analysis (Mastersizer 2000, Malvern Panalytical; Malvern, UK). Prior to analysis, 0.5 to 0.6 g sub-samples of sediment were treated with a 5% sodium hexametaphosphate solution and agitated for 5 minutes in an ultrasonic bath to disperse particles and prevent agglomeration. The event particle size distributions were assumed to be representative of the stream's suspended load as storm events contribute the majority of the total sediment flux. The proportions of particles <63 µm in diameter in the samples were averaged and combined to estimate the flux of silt and clay leaving the catchment.

2.6.4 Multi-parameter water quality sondes

Water temperature, electrical conductivity, pH, ammonium, turbidity, and dissolved oxygen were monitored at hourly intervals at 3 sites using YSI EXO2 multi-parameter sondes at hourly intervals. One sonde was deployed as part of Thames Water's 'Smarter Water Catchments' initiative between P5 and P6/P7 (Figure 3). A further sonde was deployed by the EA at TH. These sondes operated using a pumped flow cell system which minimised sensor fouling. A further EA sonde was deployed downstream of the scope of this monitoring report and did not use a pumped system, from which the data have not been used.

2.7 FSA water levels and volumes

Water levels were monitored in 12 bunds and 1 online pond (Figure 3). Rugged Level TROLL 100s were installed in stilling wells adjacent to stage boards in the deepest part of each FSA (Figure 6), surveyed using RTK-GNSS equipment. FSA Rugged level TROLL data were corrected to mASL, for atmospheric pressure and quality controlled using the same methods as described for the in-stream Rugged level TROLLs in Section 2.3.

Figure 6: Example bund monitoring site (P3), showing stilling well containing Rugged TROLL 100 pressure sensor, mounted to wooden stake and RTK-GNSS surveyed stage board in deepest part of bund.

FSA storage volume was estimated for each feature using a Digital Elevation Model (DEM), produced using 1 m horizontal resolution LiDAR data. Where no LiDAR data were available as-built manual survey data interpolated using the Natural Neighbours method were used. The vertical resolution of the LiDAR and the manual survey data are both down to micrometre resolution, however the errors are larger than this. We estimate the relative height error (random error) to be no more than ±5 cm. EA specifications require the absolute height error to be less than ±15 cm. This is the root mean square error, which quantifies the error or difference between the Ground Truth Survey and LIDAR data.

The DEMs were imported into ArcGIS to identify the maximum static water level, defined by the lowest elevation point on top of the bund. In ArcGIS the maximum FSA volume was estimated using a raster between this maximum static water level and the elevation at which the stream channel and FSA are not connected. A depth-area-volume toolset was applied to the raster to produce a depth-stored volume lookup table for each FSA.

The continuous corrected and quality-controlled water level time-series in each FSA was then used to produce a time-series of stored volume for each FSA, by matching the water level time-series to the depth-stored volume lookup table produced from ArcGIS. Note that this was not possible for the newer FSAs installed in the north sub-catchment, as no LiDAR or survey data were available.

2.8 Pond water quality and nutrient attenuation

The quality of the ponds was observed using water samples taken from the inflow and outflow (for suspended sediments, nutrients, and major anions) during storm events and baseflows. Changes in nutrient concentration as water flows through the three online ponds were observed to understand to what extent they were attenuated both during storm events and baseflow conditions. Pond outflow discharge was measured on two occasions using salt dilution gauging for lower flows, and also an electromagnetic current meter and the area-velocity method when the stream was deep enough to do so. Multi-parameter sondes were installed in one of the on-line ponds and at a downstream location to continuously measure temperature, dissolved oxygen (DO), electrical conductivity (EC), and chlorophyll.

The following methods form part of a journal paper (Robotham et al., 2021) which details the sampling of the water quality and nutrient attenuation effect of the on-line ponds.

To monitor water quality outside of storm events (i.e. under baseflow conditions), water samples from the on-line pond system's inlet and outlet were collected during field visits every 2–4 weeks. One unfiltered 60 mL sample was taken for total phosphorus (TP), and two 60 mL samples were immediately filtered through a 0.45 µm cellulose nitrate membrane (Whatman™ WCN grade; Maidstone, UK) for analysis of total dissolved phosphorus (TDP), soluble reactive phosphorus (SRP), and dissolved major ions (NO_2^-, NO_3^-, NH_4^+, F^-, Cl^- and SO_4^{2-}). Particulate phosphorus (PP) was taken to be the difference between TP and TDP.

Approximately 500 mL was sampled using the US DH-48 sampler for determination of SSC and VSC. Water chemistry samples were refrigerated at 4°C in the UKCEH labs upon return from the field until they were analysed following Wallingford Nutrient Chemistry Laboratories procedures described in detail by Bowes et al. (2018). SSC was determined gravimetrically by filtering known volumes of water samples through pre-ashed, dried and weighed Whatman™ GF/C™ filter papers, which were then oven dried at 105°C for at least two hours. Filter papers were then reweighed after cooling in a desiccator for 30 minutes. VSC was then determined through loss-on-ignition (LOI) by igniting filter papers in a muffle furnace (AAF 1100, Carbolite Gero; Hope, Derbyshire, UK) at 500°C for 30 minutes before being cooled and reweighed.

For monitoring storm events, automatic samplers (Sigma SD900, Hach; Loveland, CO, USA) were deployed and triggered between March 2019 and February 2020 at four locations along the stream to sample water flowing into and out of each pond (Figure 7). Triggering of samplers was determined based on the rainfall forecast in order to capture samples approximately representative of the event. Grab samples of run-off were taken from contributing overland flow pathways. Samples were refrigerated upon return to the laboratory, and 60 mL subsamples were taken as soon as possible for chemical determinands of interest. To ensure representative subsampling, samples were thoroughly mixed before immediately taking an aliquot using a syringe. The remaining sample was used to determine SSC and VSC using consistent methods.

Discharge was estimated at the ponds' outflows in higher flows using an Electromagnetic Current Meter (Valeport; Totnes, UK) and the velocity-area method, and also under low flows using a conductivity sensor (EXO1, YSI; Yellow Springs, OH, USA) and the salt dilution method. During storm events, run-off frequently overwhelmed the small stream channel and rendered it unsuitable for accurate flow measurement or development of a reliable stage-discharge relationship. Instead, water flowing through the ponds was estimated as a catchment area-weighted proportion of the discharge measured at a more stable gauging site (CM). In order to represent timings of storm hydrographs more realistically, the estimated discharge was shifted back in time by applying a linear regression ($R^2 = 0.51$) between peak discharge and the time difference between peak stage in the Central Pond and at the CM site. It was assumed that at a given time, discharge was equal at both pond inflows and outflows.

Figure 7: Automatic water sampler at the inlet of an on-line pond.

A multi-parameter sonde was installed in the central on-line pond next to the water level sensor and stage board. A second sonde was deployed at an instream location in the reach adjacent to the P8 storage feature. Both sondes logged temperature, dissolved oxygen (DO), electrical conductivity (EC), and chlorophyll at 15-minute intervals. Sondes were equipped with wipers which cleaned the sensors in-between measurements. Individual sensors were calibrated according to EA National Water Quality Instrumentation Service protocols. The draining and significant reduction in water level of the on-line pond in drier conditions meant that sensors were exposed to the air for periods of time. Lowering the sonde deeper into the water to avoid this also posed risks of sensor burial and fouling due to the accumulation of sediment in the pond. Consequently, water and sediment sampling yielded a more reliable source of data in this context.

2.9 Pond sediment and associated nutrient accumulation

Siltation traps were deployed in each of the on-line ponds to quantify sediment, organic matter, and P accumulation, and determine the particle size distribution of the trapped material. Ponds were also surveyed to estimate the total volume and mass of stored sediment accumulated since their construction.

The following methods form part of a journal paper (Robotham et al., 2021) which details the sampling of the sediment, organic matter, and P trapping effect of the on-line ponds.

The net accumulation of sediment and nutrients was determined in the on-line ponds using siltation traps (Figure 8).

Figure 8: Siltation trap filled with on-line pond sediment after being deployed for circa one month.

Traps were assembled from circular plastic saucers (19 cm in diameter, 4 cm in height) with weights attached to allow them to sink and rest on the pond bed. Traps were positioned in ponds as evenly as possible, with one central trap and four outer traps. The traps were deployed for periods of up to 50 days before being retrieved, emptied and immediately redeployed. Collected sediment (including pond water pooled on the surface) from each trap was emptied into individual plastic bottles for transport back to the UKCEH laboratory. Bottles were then emptied into larger plastic boxes and refrigerated for at least 48 hours to allow suspended solids to settle out. The supernatant was then siphoned off into bottles and filtered to account for the mass of any fine particles still in suspension. Sediment in the boxes was stirred thoroughly, and for each, three sub-samples of approximately 5 grams were transferred into centrifuge tubes for particle size analysis (method as described in Section 2.6.3. To determine sediment mass, the remaining sediment was distributed into pre-weighed aluminium trays (~100 g sediment per tray) and oven-dried at 105 °C for at least 48 hours before being cooled and reweighed. To determine volatile solids (organic matter proxy) by LOI, one tray per trap was then ignited at 500 °C for 2 hours before being cooled and reweighed. One tray per batch was reheated and reweighed to ensure that the sample mass remained stable and the

LOI was complete. P content was determined by grinding the ignited sample into a fine powder, of which triplicate subsamples of 3 ± 0.1 mg were taken, mixed with 60 mL ultrapure water and then analysed with the same TP methodology used for water samples (Section 2.8). Length and width transects of pond sediment depths were surveyed in January and July 2020 following a standard method, and spatially interpolated in a GIS (ArcMap, Esri; Redlands, CA, USA) using the natural neighbour interpolation method to estimate the total stored sediment volumes in each pond.

Siltation trap monitoring of the on-line ponds took place between August 2019 and March 2020 with six deployment periods. This monitoring was unable to continue beyond March 2020 due to the COVID-19 pandemic.

2.10 Bund sediment accumulation

The accumulation of sediment (and phosphorus and organic carbon) was monitored using two approaches. Sediment deposition pins were placed at regular intervals within FSAs in order to regularly measure the depth of accumulated sediment across the area. The second approach involved the collection of sediment cores to quantify bulk density, in combination with the surveying of accumulated sediment depths across bunded areas to estimate stored sediment volumes, and from this derive estimates of the stored masses.

The following methods form part of a journal paper (Robotham *et al.*, under review) which details the determination of the accumulation of sediment, organic matter, and P within offline storage features.

The deposition pins consisted of plastic-coated metal rods (approximately 1.2 m in height) that were driven into the solid ground base within the bunded area of each storage feature (Figure 9). Pins were arranged in a cross-shaped formation spanning the width and length of the bunded area, making sure to include the deepest section (typically co-located with stage board level sensor). Pins were placed at between 1 and 5 m intervals depending on the size of the bunded area. At periods of ~2 months, the height of the pins above the sediment surface was measured to determine the accumulation (or erosion). Unfortunately this approach did not yield satisfactory results for several reasons. In some features (e.g. P11) the pins were disturbed by livestock when they were dry, and in one case (P3) pins were vandalised. The rapid draining of many FSAs also meant the soil underwent frequent cycles of wetting and drying which destabilised the pins, causing them to lean in places. The degree of error associated with these issues was greater than the extent of the sediment accumulation within these ~2-month periods, rendering them unsuitable for measuring the effectiveness of the NFM features at trapping sediment in this context.

Figure 9: Erosion pins following installation in P6.

The approach that used a combination of sediment core sampling and sediment depth surveying was able to provide a more consistently successful approach across all of the NFM storage features.

Sediment cores were sampled within each FSA to determine the average bulk density of accumulated sediment. A coring device suitable for sampling soft, submerged sediment was made from 1 m long copper pipe (2.6 cm in diameter), cut at a 45° angle on one end to aid insertion into the sediment. Six cores were taken from each storage feature (half in shallower sections closer to feature margins, and half in deeper central sections). Sediment depth (down to the solid base of the storage feature) was also measured at each coring location to determine the original core length prior to any potential compaction that occurred during coring. Cores were stored in plastic sample bags and refrigerated at 4°C before being transferred into aluminium trays and oven-dried at 105°C for at least 36 hours before being weighed. Dry bulk density was calculated following guidance of Wood (2006). LOI was quantified as a proxy measure for organic matter (OM) content. The samples were heated for 2 hours at 500°C before being cooled in a desiccator and re-weighed. OM was converted into organic carbon (OC) content using a 0.58 conversion factor chosen based on the literature (Bhatti and Bauer, 2002; De Vos et al., 2005; Rollett et al., 2020). The TP concentration of the sediment was determined spectrophotometrically. The ashed sample was crushed into a fine powder and combined into a bulk sample for each storage feature from which triplicate sub-samples of 3±0.1 mg were then taken for determining average TP content. Sub-samples were mixed with 20 ml ultrapure water and analysed following the modified molybdenum blue methodology of Eisenreich et al. (1975).

Alongside the cores, additional sediment was sampled for determining the absolute particle size distribution using the methods described in Section 2.6.3.

Depths of accumulated sediment within each storage feature were surveyed along two transects spanning the length and width of the feature, with measurements being taken at 1 to 2 m intervals. Depths were measured from the solid base of the feature to the surface of the soft sediment layer using a metre rule. Transects were positioned so that they approximately captured the deepest section of the storage feature and a handheld GPS (eTrex, Garmin; Olathe, KS, USA) was used to locate the start and end points of each transect. Maintenance work to remove sediment from the series of P10 ponds following their surveying in January and June 2020 meant that any future surveying would not represent the accumulation since construction. As a result, sediment depths measured for these features represent a shorter period of accumulation compared to the other features which were measured following a longer period post-construction and with no maintenance. Sediment depths were spatially interpolated using the natural neighbour interpolation method (ArcMap 10.5, Esri; Redlands, CA, USA) to estimate stored sediment volumes. The bulk density measurements were then used to convert sediment volumes into masses, and concentration data were used to calculate total stored nutrient masses. A combination of LiDAR and RTK GNSS (GS14, Leica Geosystems; St. Gallen, Switzerland) surveys of the features post-construction were similarly used to estimate their total storage volumes.

3 Data Coverage

Total data coverage for the monitoring period is over 90% across all sensors. Monthly data coverage is shown in Figure 10 for the sensors and combined parameters used for analyses within this report.

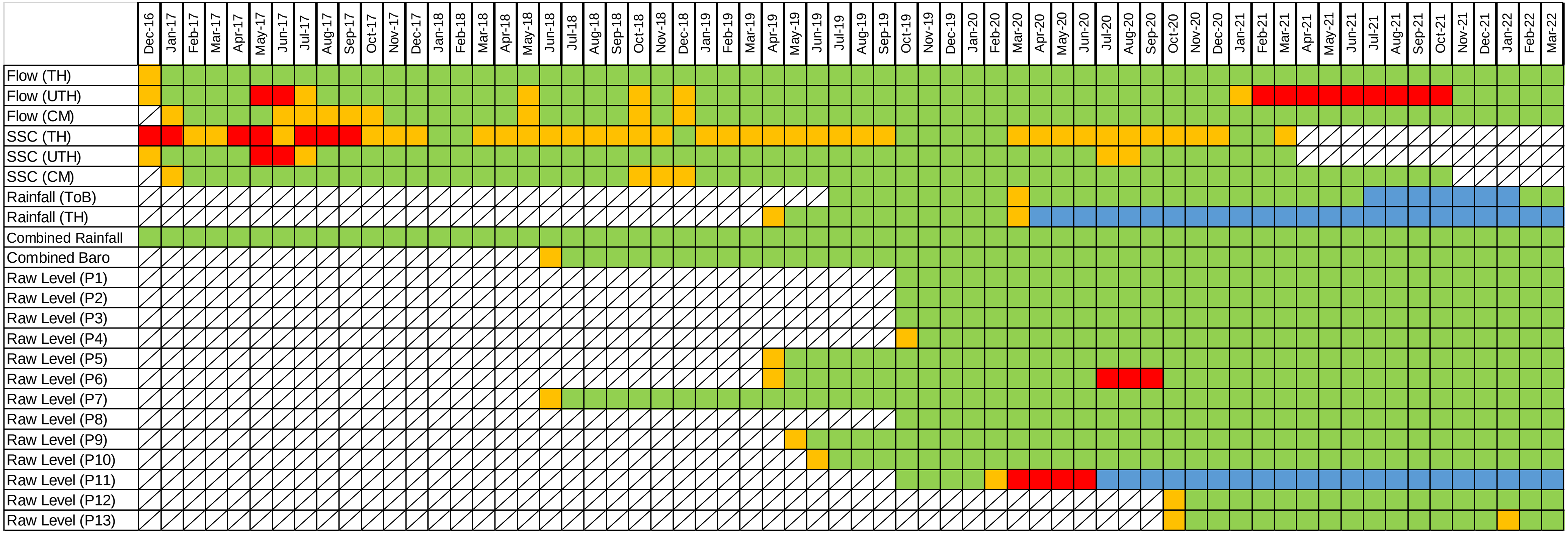

Figure 10: Monthly data coverage for parameters and sensors over Littlestock Brook NFM trial. Green = >90% data coverage, amber = <90% data coverage, red = no data, blue = suspect data. NB: P1 in this table is also referred to as OLP1 and P1_OLP in different report sections, to keep consistent with linked publications. In this table, P10 refers to the second pond within the series of three online ponds (as shown in Figure 3). This was the only instrumented pond in the series. This pond is also referred to as OLP10, P10_OLP and Central Pond in different report sections, to keep consistent with linked publications.

3.1 Flow

Figure 10 shows flow 100% data coverage at TH for the monitoring period, with the exception of December 2019 when the first sensor was installed at this site. Data coverage at UTH has some months of <90% data coverage and no data periods due to technical issues with the sensor at that time. From January 2021 there is an extended period of no data due to the sensor coming to the end of its lifespan; it was then replaced at the start of November later that year. Some data from the old sensor may be recoverable by the manufacturer a later date. Flow data at CM had several periods of <90% coverage due to issues with the sensor. This was eventually replaced in October 2017 to give more consistent data coverage for the rest of the monitoring period.

3.2 Suspended Sediment Concentration

Overall the SSC data show good coverage for the majority of the monitoring period, however due to the optical nature of the turbidity sensors, data gaps and issues typically occur more frequently compared to other data collection methods. Figure 10 shows that SSC data coverage at TH is notably patchy for the first year of monitoring until December 2017, when the additional multi-parameter water quality sonde (measuring turbidity) was installed. The data coverage issues in this early period relate to the low water levels at this hydrologically flashy site resulting in the sensor being above the water level most of the time (except during rainfall events). Data coverage is more complete at the UTH site with the exception of two summer months in 2017 missing due to a technical issue with the datalogger. The CM site has the most complete series of data, with only 4 months of <90% data coverage due to issues with the turbidity probe at this site.

3.3 Rainfall

Figure 10 shows that overall the combined rainfall coverage for the Littlestock Brook area is 100% due to the multiple sources of data used to form this data series. The ToB and TH rain gauges were installed in 2019 and have good coverage until March 2020 when some of the data were lost as a result of data being automatically overwritten during the Covid-19 lockdown period. The period of suspect data for the ToB site is as a result of the tipping bucket becoming blocked. The period of suspect data at TH site is as a result of the gauge becoming unstable and potentially out of calibration. During these periods, Little Rissington rainfall data were used to ensure reliability as detailed in Section 2.2.

3.4 Atmospheric Pressure

The combined barometric pressure data coverage in Figure 10 shows 100% data coverage for the monitoring period. There is <90% data in the installation month as the sensor was installed mid-month. This combined time-series is the pressure sensor in the barn Grange Farm with missing or suspect atmospheric pressure data infilled or corrected using either the back-up barometric sensor located at the Heath or from the Met Office Little Rissington data, as detailed in Section 2.3. This is the time-series that was used to correct stream and FSA water level data.

3.5 FSA water levels

FSA P1-13 data coverage in Figure 10 is for raw sensor data, as FSAs frequently dry out resulting in prolonged no data during dry periods. Across all sensors over 98% of total data coverage was achieved. Less than 90% data coverage is observed for most FSAs in sensor installation months as the whole month was not monitored. There is missing P6 data for the period July to October 2020 due to a sensor error. The P11 sensor was repeatedly knocked over during strong flood events and by livestock, resulting in missing or suspect data from February 2020 onwards. This is as the replacement sensors were not surveyed before being knocked over again. The P13 sensor was knocked over by livestock in January 2022, this was recovered and replaced during the same month resulting in less than 90% data coverage.

4 Analysis

4.1 Rainfall

Daily rainfall totals for the area are presented in Figure 11 with the antecedent precipitation index (API) giving an indication of catchment wetness over the period. The trend-line shows how the winters in 2020 and 2021 were notably wet, with the highest daily total exceeding 40 mm on 23rd December 2020. Having higher API values prior to intense rainfall events increases the risk of rapid run-off responses. Under these conditions NFM may be particularly valuable in delaying and attenuating this response. The drought conditions that occurred during summer 2018 can be clearly seen reflected in the API which drew down close to 0.

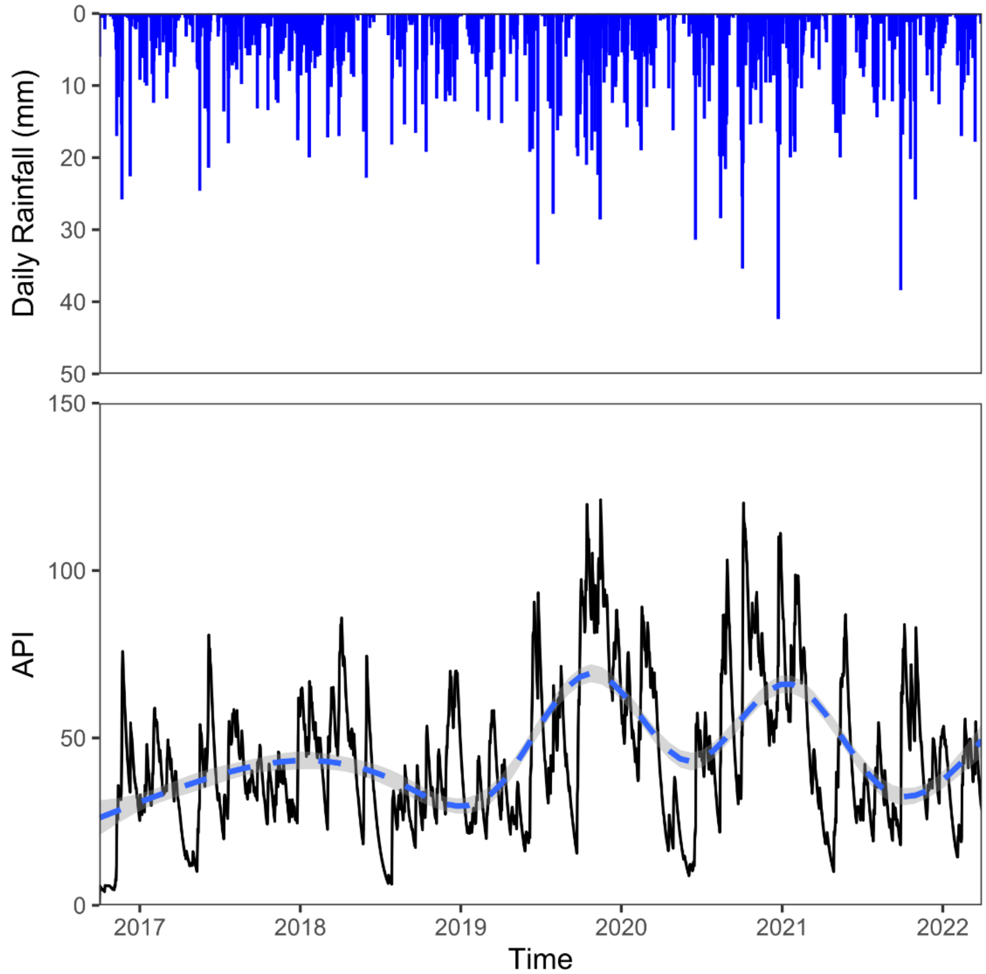

Figure 11: Daily rainfall totals (mm) and Antecedent Precipitation Index (API) from October 2016 to April 2022.

Table 8 gives the total annual rainfall in each water year. The water year for 2017 (prior to implementation of NFM) was notably dry when compared to the 30-year (1991-2020) average of 809.6 mm (Met Office, 2022). This contrasts to the particularly wet years of 2020 and 2021 following NFM implementation.

Table 8: Total annual rainfall (mm) for each water year in the monitoring period. 2022 total includes up to April 1st.

Water Year	Total Rainfall (mm)
2017	674.2
2018	686.2
2019	800.6
2020	988.2
2021	965.0
2022†	359.2

†Years with incomplete data (see Figure 10, Section 3 'Data Coverage').

4.2 Annual stream discharge

Stream discharges (flows) are presented at 5-minute resolution for each water year (1st October – 30th September) at each of the three streamflow monitoring sites (Figure 12; Figure 13; Figure 14). It is important to note that for the UTH site, only discharges up to 330 L s^{-1} are displayed due to the uncertainty in the stage-discharge rating above this threshold at this site.

Church Meadow:

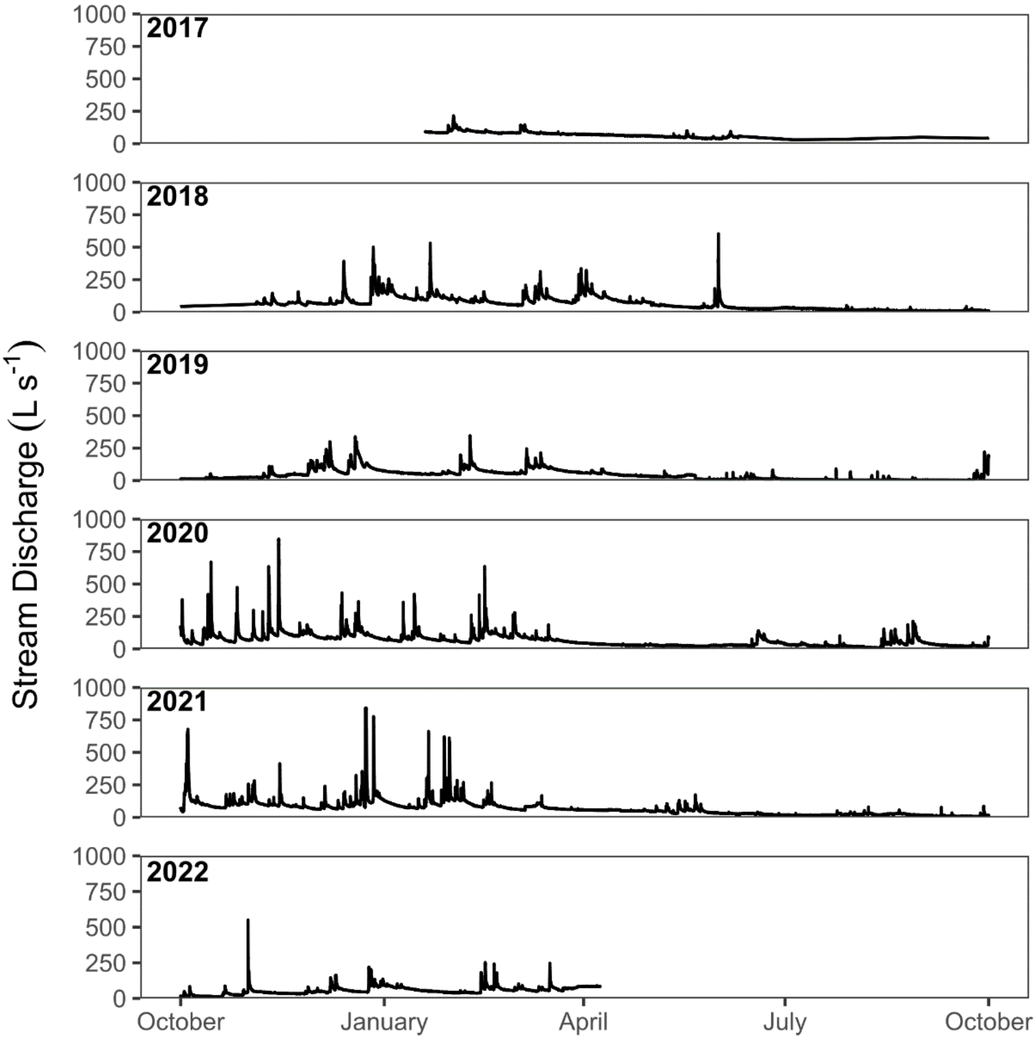

Figure 12: Stream discharge (L s-1) at Church Meadow (CM) in each water year of the monitoring period. The data series starts in January 2017 and ends in April 2022. NB. Y-axis scale is lower than North Catchment (TH and UTH) plots (Figures 13 and 14) to show full detail.

The Heath:

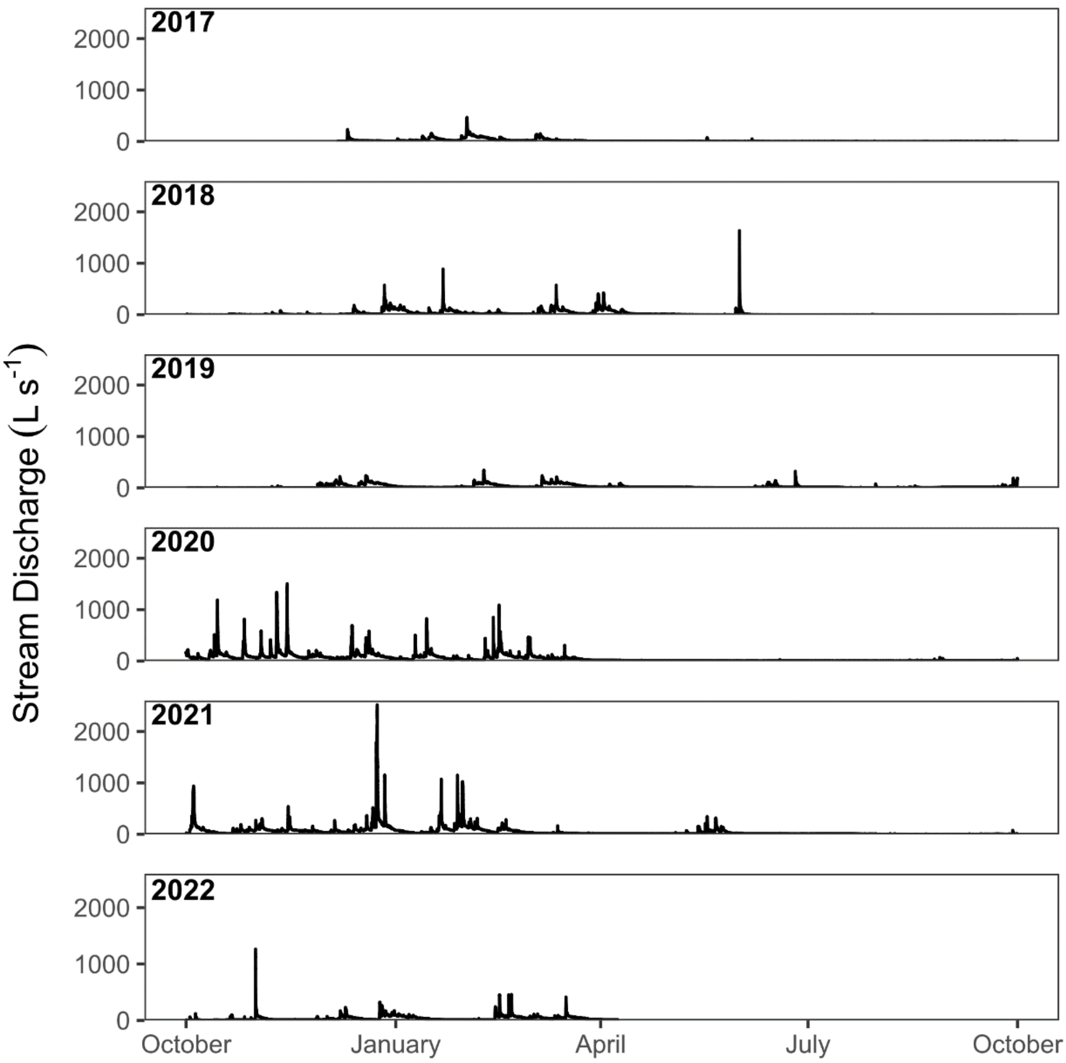

Figure 13: Stream discharge (L s^{-1}) at The Heath (TH) in each water year of the monitoring period. The data series starts in December 2016 and ends in April 2022. NB. Y-axis scale goes beyond that of CM in the South sub-catchment (Figure 12).

Upstream The Heath:

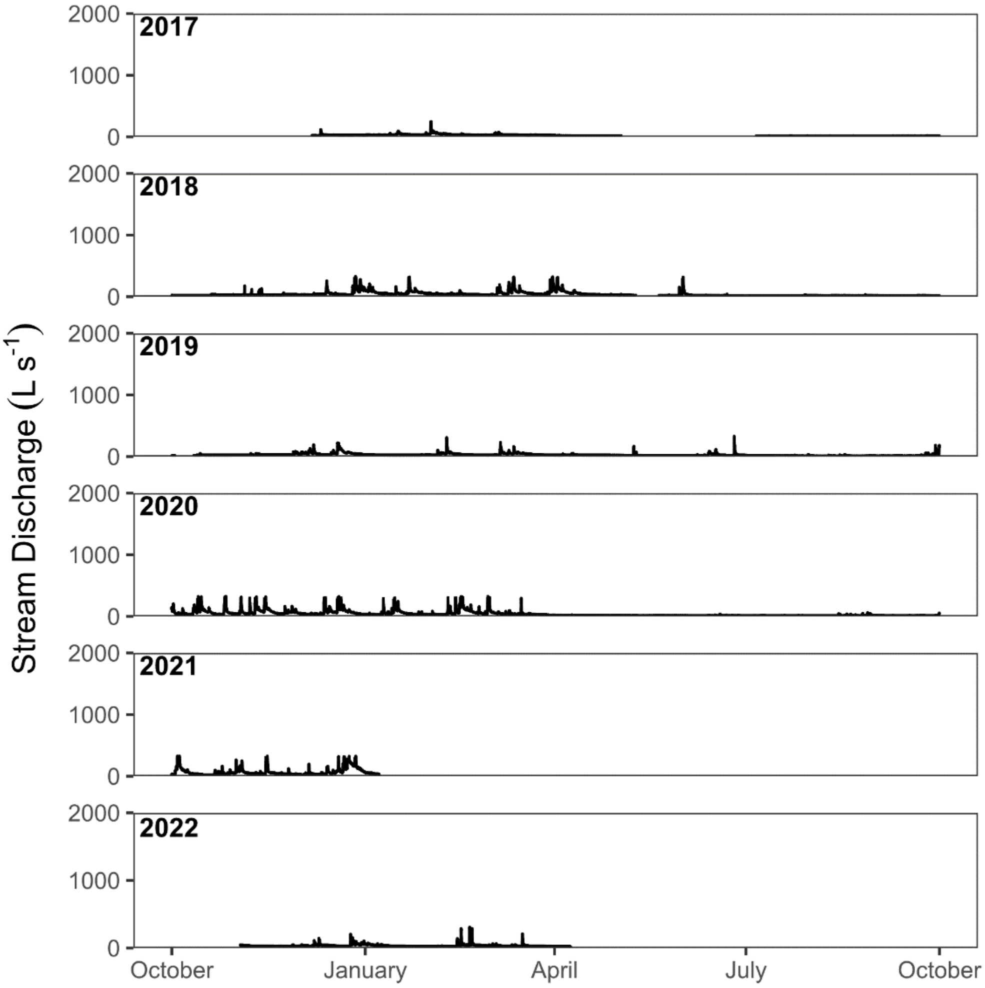

Figure 14: Stream discharge (L s^{-1}) at Upstream The Heath (UTH) in each water year of the monitoring period. The data series starts in December 2016 and ends in April 2022. NB. Y-axis scale goes beyond that of CM in the South sub-catchment (Figure 12).

Table 9 shows the total annual discharge (water flux) leaving each of the monitored sub-catchments for each water year. Despite considerably higher storm event peaks in the North sub-catchment, the total discharge was consistently higher from the South sub-catchment, reflecting its higher baseflow component influenced by a potentially larger sub-surface (groundwater) contributing area.

Table 9: Total annual discharge (million m^3) from the North and South sub-catchments during each water year.

Total Discharge (million m^3)		
Water Year	Sub-catchment	
	North	South
2017†	0.365	1.310
2018	0.646	2.075
2019	0.712	1.363
2020	1.626	2.116
2021	1.532	2.197
2022†	0.600	0.922

†Years with incomplete data (see Section 3 ‘Data Coverage’).

4.3 Annual fluxes of suspended sediment and nutrients

SSC is presented at a 5-minute resolution for each water year (1st October – 30th September) at each of the three SSC monitoring sites (Figure 15; Figure 16; Figure 17).

At CM, SSC was relatively low (<1000 mg L^{-1}) during the dry year of 2017. The 2021 water year was notably rich in events of high SSC reflecting the wet conditions that occurred early on in the autumn when arable fields were still largely bare.

Church Meadow:

NB. Data after January 2021 during storm events is truncated due to the sensor used from this point onwards having an upper measurement limit of ~1600 mg L^{-1}. Beyond this point event peaks are missed in instances where turbidity exceeded this.

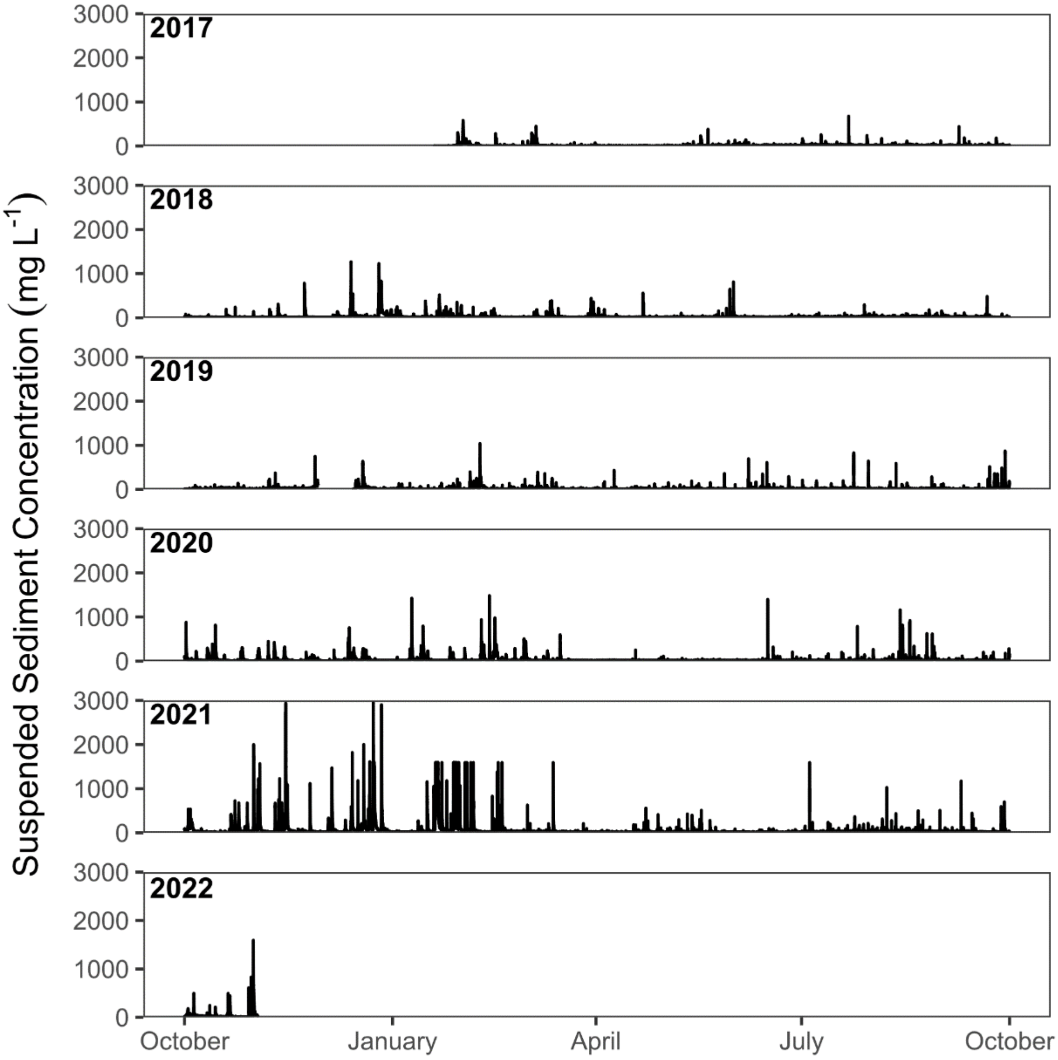

Figure 15: Stream suspended sediment concentration (mg L^{-1}) at Church Meadow (CM) in each water year of the monitoring period. The data series starts in January 2017 and ends in October 2022.

SSC at TH had a particularly flashy response mirroring the hydrological regime of this sub-catchment. Measured SSC was highest at this site and frequently exceeded 1000 mg L^{-1}, even reaching relatively high concentrations during the dry year of 2017.

The Heath:

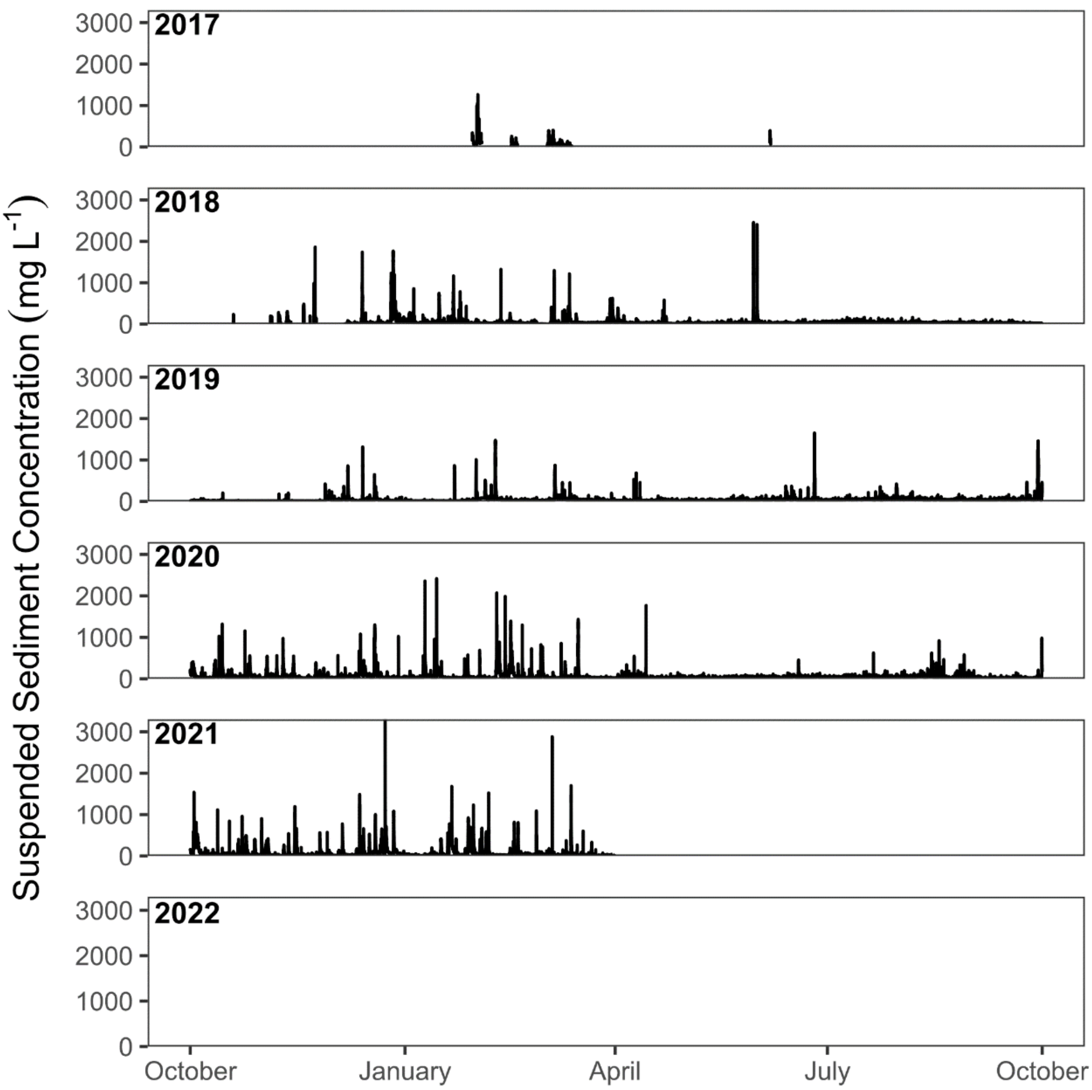

Figure 16: Stream suspended sediment concentration (mg L^{-1}) at The Heath (TH) in each water year of the monitoring period. The data series starts in February 2017 and ends in April 2021.

SSC at UTH is similar to TH in its response but has overall lower concentrations. This suggests that there are significant sources of sediment entering the stream between UTH and TH. Potential critical source areas are likely to include the incised and largely unvegetated channel banks in the reach just upstream of TH and the adjacent arable field.

Upstream The Heath:

Table 10, Table 11 and Table 12 show the fluxes of suspended sediment, total phosphorus, and particulate organic carbon leaving the monitored sub-catchments in each water year.

Table 10: Suspended sediment flux (tonnes) and lower/upper uncertainty bounds in round brackets from the North/South sub-catchments during each water year. Values in square brackets show fluxes for periods that do not span the full water year, to allow sub-catchment comparison.

Suspended Sediment Flux (t)		
Water Year	Sub-catchment	
	North	South
2017†	29.99 (27.05 – 32.93)	24.42 (22.58 – 26.30)
2018	112.45 (96.03 – 128.82)	101.40 (93.88 – 109.11)
2019†	60.34 (54.50 – 69.57)	48.69 (44.13 – 53.48)
2020	259.09 (232.23 – 288.25)	135.29 (129.30 – 141.37)
2021†	[280.31 (251.44 – 311.34)]	358.26 (341.12 – 375.79) [344.85 (328.40 – 361.72)]

†Years with incomplete data (see Section 3.2 'Data Coverage').

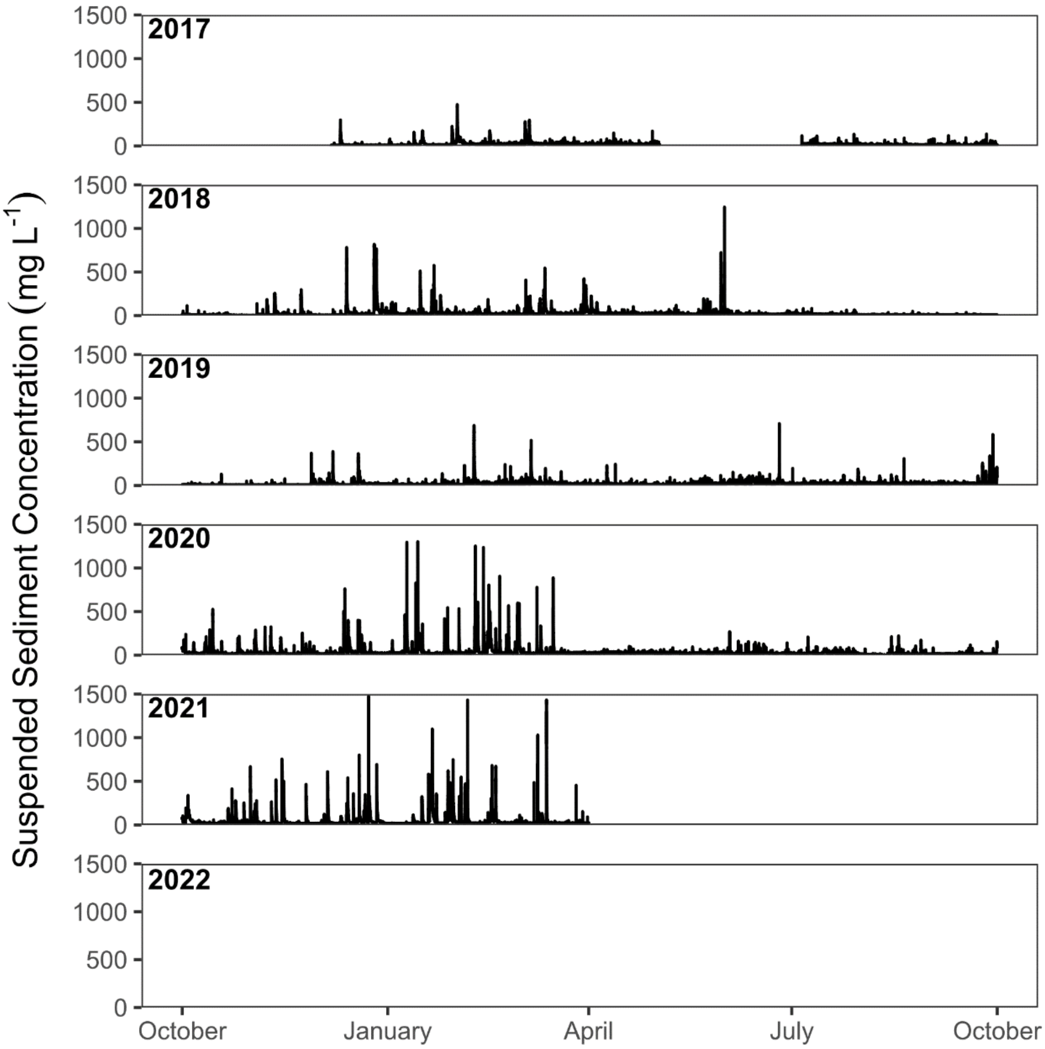

Figure 17: Stream suspended sediment concentration (mg L^{-1}) at Upstream The Heath (UTH) in each water year of the monitoring period. The data series starts in December 2016 and ends in April 2021.

Table 11: Total phosphorus flux (kg) from the North/South sub-catchments during each water year. Values in brackets show fluxes for periods that do not span the entire water year to allow sub-catchment comparison.

Total Phosphorus Flux (kg)		
Water Year	**Sub-catchment**	
	North	**South**
2017†	107.02	92.23
2018	304.16	265.30
2019†	214.31	135.20
2020	719.96	331.10
2021†	(725.02)	757.58 (714.72)

†Years with incomplete data (see Section 3.2 'Data Coverage').

Table 12: Particulate organic carbon flux (tonnes) from the North/South sub-catchments during water years. Values in brackets show fluxes for periods that do not span the entire water year to allow sub-catchment comparison.

Particulate Organic Carbon Flux (t)		
Water Year	**Sub-catchment**	
	North	**South**
2017†	2.57	2.46
2018	9.63	10.20
2019†	5.17	4.90
2020	22.18	13.61
2021†	(24.00)	36.05 (34.70)

†Years with incomplete data (see Section 3.2 'Data Coverage').

Suspended fluxes of sediment, total phosphorus and organic carbon show broadly similar patterns across the observed water years. Fluxes varied greatly between the years, largely reflecting the changing hydrometeorological conditions. Suspended sediment and POC fluxes were consistently higher from the North sub-catchment up to the 2020 water year. However in 2021 the fluxes were higher from the South sub-catchment, with the exception of TP. This is a result of the chronically elevated dissolved P component in the North sub-catchment.

4.4 Sediment and nutrient accumulation in FSAs

The ability of the FSAs to trap sediment and associated nutrients was assessed through multiple monitoring methods with varying degrees of success. The key findings presented within this report section are taken from a research article currently under review in the *Earth Surface Processes and Landforms* journal (Robotham et al., 2022a).

<u>Sediment and nutrient storage:</u>
The accumulated masses estimated from the sediment depth surveying and core sampling are given in Table 13. The total sediment, TP and OC captured by the FSA and pond features varied by two orders of magnitude, ranging from 0.2 to 20.1 tonnes of sediment during the 2 to 3 years since construction. Bulk density of the accumulated sediment had a mean of 0.69 ± 0.23 g cm^{-3} for online features and 0.93 ± 0.22 g cm^{-3} for offline features. Cumulatively, the 13 features within the south sub-catchment stored 83 tonnes of sediment with a total volume of 108.8 m^3. The FSAs were most effective in trapping sediment, with 14.7% of the total sediment flux and 14.1% of the fine (clay and silt) sediment flux stored compared to only 9.5% and 7.5% of the TP and POC fluxes respectively.

Table 13: Fluxes (±95% CI), masses of accumulated sediment (t), Total Phosphorus (kg), and Organic Carbon (t) in storage features and their equivalent proportion of the total suspended sediment, fine suspended sediment, TP, and particulate OC fluxes leaving the 3.4 km^2 South sub-catchment.

Storage Feature	Time period	Rainfall (mm)	Total sediment flux (t)	TP flux (kg)	POC flux (t)	Stored sediment (t)	Stored TP (kg)	Stored POC (t)	Total sediment flux stored (%)	Fine sediment flux stored (%)	TP flux stored (%)	POC flux stored (%)	Sub-catchment area drained (%)
P0_OLP	Feb 19–Mar 21	2126	498±24	1095±50	50±1	5.8	8.0	0.3	1.2	1	0.7	0.6	12.1
P1_OLP						6.2	14.4	0.4	1.3	1.4	1.3	0.8	9.0
P2						0.4	0.5	0.03	0.07	0.06	0.04	0.06	0.3
P3						20.1	28.9	1.1	4.0	3.7	2.6	2.2	0.1
P4	Feb 18–Mar 21	2810	565±30	1278±65	57±2	0.3	0.4	0.01	0.05	0.05	0.03	0.02	1.1
P5						7.0	11.0	0.3	1.2	1.3	0.9	0.5	1.2
P6						8.7	14.2	0.4	1.6	1.8	1.1	0.7	1.9
P7						10.6	16.7	0.4	1.9	2.1	1.3	0.7	2.8
P8						0.2	0.2	0.01	0.03	0.04	0.02	0.02	0.3
P9						0.6	0.6	0.02	0.1	0.1	0.05	0.03	5.9
P10_OLP	Feb 18–Jan 20	1634	160±10	417±26	16±1	4.6	5.5	0.2	2.9	2.5	1.3	1.3	8.8
P10_US_OLP						10.7	13.1	0.8	6.7	4.6	3.2	5.0	
P10_DS_OLP	Feb 18–Jun 20	1944	207±12	533±30	21±1	7.8	8.5	0.3	3.8	3.6	1.6	1.4	
P11_OLP	Feb 19–Mar 21	2126	605±102	1614±250	52±6	3.8	5.9	0.2	0.6	0.7	0.4	0.4	0.2
Total†		2810	565±30	1278±65	57±2	83.0	121.8	4.3	14.7	14.1	9.5	7.5	43.5

†Total excludes P11_OLP as this feature is in the North sub-catchment.

NB. P1_OLP is also referred to as OLP1 and P1 in different report sections, to keep consistent with linked publications. The three P10_OLPs are also referred to as Upstream, Central and Downstream ponds in Section 4.5 and as one entity as OLP10, P10 and elsewhere in the report, to keep consistent with linked publications.

Factors influencing accumulation rates:

Hydrology

The hydrology and filling of the different FSAs and ponds is notably varied, with some features being permanently ponded and thereby always having an antecedent storage component. On the other hand, some features only fill during rainfall events and then drain down and dry shortly after. P3 showed the greatest retention of water with 60% of its capacity exceeded 50% of the time, equating to a median storage volume of 338 m^3. P8 filled infrequently and only ever filled to 12% (68 m^3) of its potential storage capacity during this period. P6 also had a hydrologically flashy filling regime but stored significantly more water, reaching 26% capacity (688 m^3), one order of magnitude greater than P8. In comparison P5 exhibited less flashy behaviour, sustaining water storage for a greater duration and at its peak filling to 1475 m^3, 42% of its potential capacity.

Connectivity & design

On average, the sediment accumulation rate was 3.3 times higher in on-line features (20.8 ± 9.8 kg m^{-2} y^{-1}) than in offline features (6.3 ± 5.2 kg m^{-2} y^{-1}) when taking into account the ponded area of each feature. The width-to-length ratio of features explained some of the variation in accumulation rates, with positive relationships observed for both sediment (R^2=0.42, p<0.05) and TP accumulation (R^2=0.54, p<0.01). Width-to-length ratios were generally low and ranged from ~0.25 to 2.0, with P1_OLP having the highest ratio. Contributing area was also found to positively influence sediment accumulation rate (R^2=0.49, p<0.05). Differences in accumulation rate were better explained by event contributing area which broadly clusters the offline features into those activated by leaky barriers and those that were not (Figure 18).

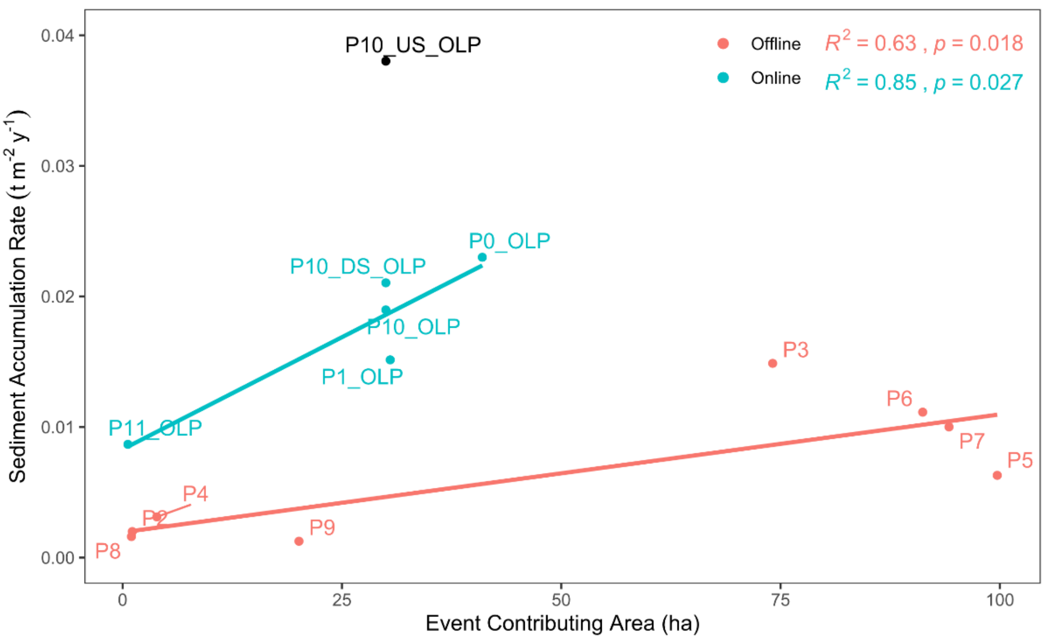

Figure 18: Linear regressions between event contributing area (ha) and sediment accumulation rate (t m^{-2} y^{-1}) for offline and online NFM storage features. P10_US_OLP is excluded from the regression.

Features such as P9 were never observed to fill from overbank flows whereas P6 was frequently observed to do so during event peaks in winter storms (Figure 19). Overbank flows by the leaky barrier and spillway connected to P6 occurred in over 20 storm events between October 2019 and March 2021. The threshold for overbank flow was never reached at the P9 spillway; even at the peak of the highest magnitude event in December 2020 the water level was still 0.3 m below the threshold. During this event, peak storage in P6 reached over double the volume in P9. The timing of overbank flow was generally well aligned with stream SSC, allowing the highest sediment load to be diverted into P6 during event peaks.

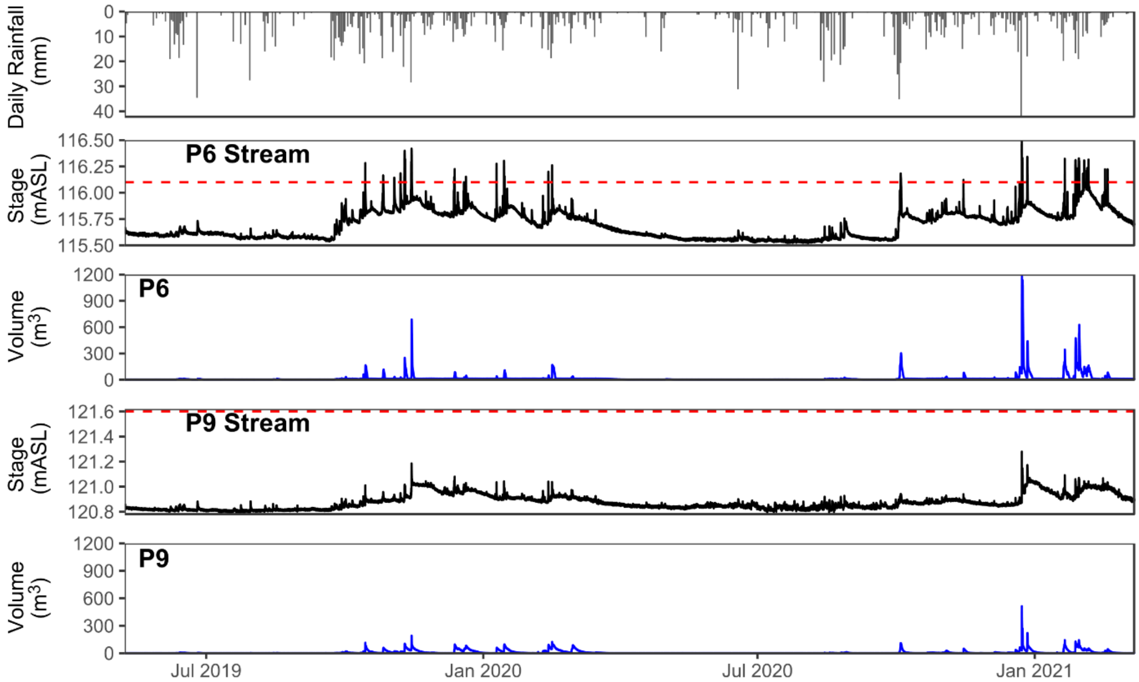

Figure 19: Time-series of daily rainfall (mm), and stream stage (mASL) at leaky barriers and water volume (m^3) in NFM storage features P6 and P9. Dashed red lines indicate the threshold at which spillways are activated. mASL = metres above sea level.

<u>Sediment enrichment:</u>

Sediments deposited within FSA and pond features were found to be significantly enriched in TP (paired samples *t*-test, p<0.01, n=14), with an average concentration 1.5 times greater than the surface soil in contributing areas. The highest TP enrichment ratio of 2.66 was observed for P1_OLP. On average the sediment was composed of 86% silt and clay particles. Enrichment of clay was typically higher in the offline features. The opposite trend was observed for sand content. In terms of OC enrichment, there were no apparent differences between the offline and on-line features.

<u>Reductions in FSA storage capacity:</u>

In the 2 to 3 years since construction, the majority of FSAs did not lose significant volumes of their maximum storage capacity as a result of sediment loading (Table 14). Average annual losses in storage capacity during the monitoring period ranged from 0.01% in P4 and P8 up to 12.9% in P0_OLP. In order to maintain their ability to fill and drain effectively during and after events, storage features require their outlets to remain sufficiently above the level of accumulated sediment, thereby helping to prevent siltation within drains. When considering the remaining storage capacity up to the drain height of features, the accumulated sediment volumes had a much greater impact. Potential storage for water and sediment is most reduced in the online features, with P10_US_OLP, P10_OLP, and P0_OLP all predicted to fill beyond their outlet drain heights within 10 years (based on current accumulation rates). Whilst having a high accumulation rate, at a 10-year timescale P1_OLP is predicted to still retain >50% of its storage capacity up to its outlet. P1_OLP with its deeper design had a mean water depth of 0.71 m during autumn and winter in contrast to only 0.3 m in P10_OLP with its shallow design and comparatively low outlet elevation. Interestingly, loss of storage capacity in P11 was negligible due to the sediment accumulation rate being too small to quantify even after over 2 years since construction. However, P11_OLP (connected to the outflow of P11) lost almost 5% of its total storage within the same period.

Table 14: Percentage reductions in the maximum storage capacity and the storage capacity up to drain heights of FSAs since their construction. 10-year reductions in storage capacity are estimates based on the measured rates of accumulation during the monitoring period. NB. It was not possible to calculate storage capacities up to drain heights for all features.

Storage Feature	Storage capacity to drain (m^3)	Reduction in max. storage capacity (%)	Reduction in storage capacity to drain (%)	Annual reduction in max. storage capacity (%)	10-year reduction in max. storage capacity (%)	10-year reduction in storage capacity to drain (%)
P0_OLP	-	27.34	-	12.9	100	-
P1_OLP	144.01	2.95	9.00	1.39	11.4	42.4
P2	-	0.57	-	0.27	2.7	-
P3	-	4.23	-	2.00	20.0	-
P4	113.74	0.03	0.26	0.01	0.1	0.8
P5	121.93	0.19	5.40	0.06	0.6	17.3
P6	130.46	0.38	7.69	0.12	1.2	24.7
P7	310.91	0.49	4.30	0.16	1.6	13.8
P8	17.37	0.04	1.30	0.01	0.1	4.2
P9	89.55	0.07	0.72	0.02	0.2	2.3
P10_OLP	20.24	8.18	36.36	4.22	42.2	>100
P10_US_OLP	25.52	19.84	54.43	10.23	>100	>100
P10_DS_OLP	48.46	10.41	20.41	4.37	43.7	85.8
P11	-	0.00	-	0.00	-	-
P11_OLP	-	4.75	-	2.24	22.4	-

<u>Sediment deposition pins:</u>

Sediment deposition pins proved to be unsuitable for assessing the accumulation of fine sediment within the FSA and pond features for the multiple reasons listed in Section 2.10. For future monitoring programmes we recommend that sediment deposition is best quantified through surveying of sediment depths alongside core sampling to avoid issues surrounding large degrees of uncertainty that are associated with the deposition pin method. However, if deposition pins are used, they are more likely to yield meaningful results when:

- Placed within permanently wet features
- Placed within locations with soil types less prone to swelling/shrinking
- Placed away from livestock and publicly accessible areas (vandalism/removal)

4.5 Sediment and nutrient attenuation in online ponds

Detailed monitoring of the on-line ponds (P10; Tears of Bruern) allowed their effectiveness for sediment and nutrient retention to be analysed. These analyses are detailed in full in a peer-reviewed scientific journal article (Robotham et al., 2021), of which the abstract is given below and the key findings are presented within this report section.

Abstract:

The creation of ponds and wetlands has the potential to alleviate stream water quality impairment in catchments affected by diffuse agricultural pollution. Understanding the hydrological and biogeochemical functioning of these features is important in determining their effectiveness at mitigating pollution. This study investigated sediment and nutrient retention in three connected (on-line) ponds on a lowland headwater stream by sampling inflowing and outflowing concentrations during base and storm flows. Sediment trapping devices were used to quantify sediment and phosphorus accumulations within ponds over approximately monthly periods. The organic matter content and particle size composition of accumulated sediment were also measured. The ponds retained dissolved nitrate, soluble reactive phosphorus and suspended solids during baseflows. During small to moderate storm events, some ponds were able to reduce peak concentrations and loads of suspended solids and phosphorus; however, during large magnitude events, resuspension of deposited sediment resulted in net loss. Ponds filtered out larger particles most effectively. Between August 2019 and March 2020, the ponds accumulated 0.306 t ha^{-1} sediment from the 30 ha contributing area. During this period, total sediment accumulations in ponds were estimated to equal 7.6% of the suspended flux leaving the 340 ha catchment downstream. This study demonstrates the complexity of pollutant retention dynamics in on-line ponds and highlights how their effectiveness can be influenced by the timing and magnitude of events.

Highlights:

- On-line ponds significantly reduced concentrations of biologically-available nutrients on average (nitrate by 5 % and soluble reactive phosphate by 29 %).
- Overall, on-line ponds acted as a net sink of sediment despite some instances of sediment resuspension/flushing during larger storms.
- On-line ponds require frequent maintenance (approximately every 2 years) for efficient functioning.

Baseflows:

Under baseflow conditions (outside of storm events), 19 sets of water chemistry samples were taken between March 2019 and March 2020. Significant differences between inlet and outlet concentrations were found for dissolved nitrate (NO_3^-), SRP, SSC, and VSC which all showed a decrease in mean concentration at the outlet (paired samples t-test, $p < 0.01$, $n = 19$; Figure 20). Table 15 gives the average concentrations at the inflow and outflow of the on-line pond system along with the average, minimum and maximum removal efficiencies of each determinand.

Table 15: Mean (±SD) inflow and outflow concentrations (mg L^{-1}), and mean (±SD), minimum, and maximum Removal Efficiency (%) of the on-line pond system for water quality determinands sampled during baseflow conditions. Determinands that showed statistically significantly attenuation are shown in bold font.

Determinand	Mean Inflow Concentration (mg L^{-1})	Mean Outflow Concentration (mg L^{-1})	Mean Removal Efficiency (%)	Minimum Removal Efficiency (%)	Maximum Removal Efficiency (%)
SRP	0.008 ± 0.006	0.005 ± 0.004	29 ± 37	-100	74
TDP	0.041 ± 0.023	0.038 ± 0.02	3 ± 43	-117	68
PP	0.04 ± 0.04	0.052 ± 0.059	-237 ± 579	-2100	95
TP	0.081 ± 0.048	0.089 ± 0.069	-34 ± 125	-314	77
NH_4^+	0.023 ± 0.026	0.024 ± 0.025	-61 ± 118	-400	73
NO_3^-	36.56 ± 3.585	34.903 ± 4.4	5 ± 6	-2	23
F^-	0.068 ± 0.023	0.067 ± 0.024	0 ± 18	-23	35
Cl^-	16.913 ± 2.382	16.835 ± 2.045	0 ± 7	-23	14
SO_4^{2-}	17.006 ± 2.652	16.904 ± 2.488	0 ± 9	-29	18
SSC	21.2 ± 4.153	13.464 ± 6.943	32 ± 24	-17	70
VSC	7.09 ± 4.153	3.901 ± 1.469	40 ± 15	15	66

NB. Nitrite (NO_2^-) was excluded from the statistical tests due to a majority (67 %) of both inlet and outlet samples measuring 0 mg NO_2^- L^{-1}.

Under baseflow conditions removal efficiencies exhibited considerable variability between the water quality determinands. Removal ranged from extreme negative values (indicating net export from the pond system) for PP, to more consistently positive values (indicating net retention) for SSC and VSC. Overall, the majority of average removal efficiencies for the sampling period were positive, with the exceptions being PP, TP, and NH_4^+.

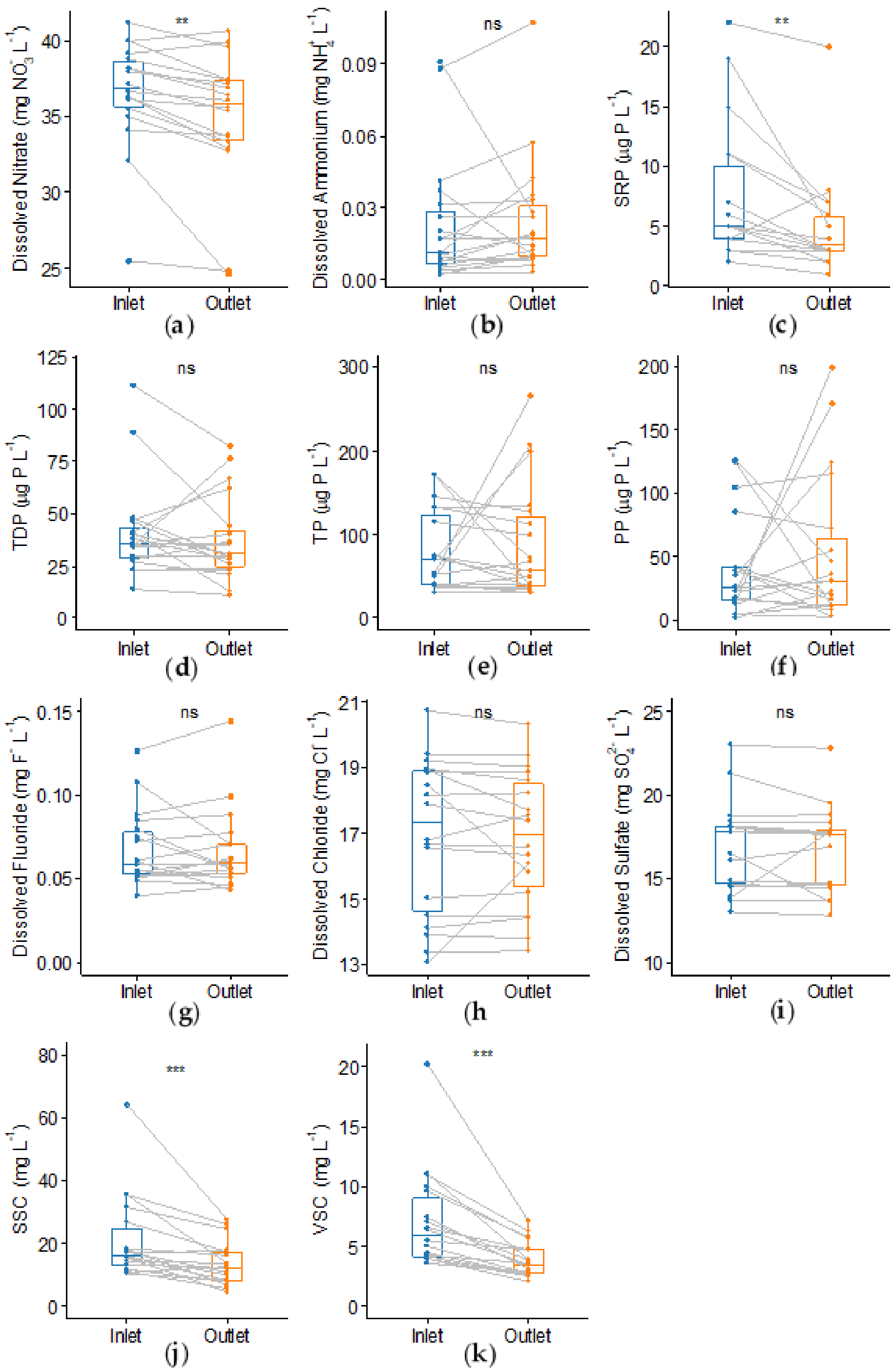

*Figure 20: Boxplots of paired on-line pond inlet and outlet concentrations for water quality determinands. Median values are represented by horizontal lines. Significance levels for results of paired samples t-tests are indicated with: *** ($p < 0.001$), ** ($p < 0.01$), ns ($p > 0.05$).*

<u>Storm events:</u>

Four storm events were captured between March 2019 and February 2020 (Table 16); however it was not always possible to trigger all four automatic samplers for every storm. The event captured in February was during Storm Dennis and had the highest rainfall (total monthly rainfall in February was 170 % above average for the area). Estimated peak discharge was highest during the November event, with an estimated return period of 5.5 years. The API gives an indication of the likely soil moisture conditions, and was found to be highest prior to the October 14th event following a rapid wetting of the catchment at the end of September.

Table 16: Mean (±SD) SSC (mg L^{-1}) for each pond monitoring site during four storm events, estimated discharge (L s^{-1}) prior to the event and at its peak, and the sampling duration (hours). Rainfall (mm) is the total event precipitation and Antecedent Precipitation Index (API) (mm) is given for the day prior to each event.

Storm Event	Mean SSC (mg L^{-1})				Sampling Duration (h)	Estimated Discharge (L s^{-1})		Rainfall (mm)	API (mm)
	Upstream Pond Inlet	Upstream Pond Outlet	Central Pond Outlet	Downstream Pond Outlet		Pre-event	Peak		
12th/13th March 2019	45 ± 47	30 ± 33	29 ± 27	35 ± 30	23	8.9	18.7	8.8	51.9
14th October 2019	258 ± 365	161 ± 152	143 ± 94	126 ± 55	5.75	8.4	58.6	23.1	104.1
14th November 2019	92 ± 67	27 ± 11	24 ± 7	-	5.75	9.2	74	31.8	97.6
15th/16th February 2020	-	87 ± 63	98 ± 79	-	23	12.3	55.7	32.2	64.8

The March 2019 event was the smallest in magnitude, with the least rainfall and lowest API, but still resulted in a peak SSC of > 200 mg L^{-1} at the inlet to the Upstream Pond, with the peak then being reduced by ~50 % downstream at the outlet of the Downstream Pond (Figure 21d). Streamflow responded rapidly to rainfall with a lag time of less than two hours (Figure 21a/4b). The response of suspended sediment was partially staggered, with lag times increasing downstream at each monitoring point except for water leaving the Downstream Pond which peaked simultaneously with water leaving the Central Pond. SSC at the Downstream Pond outlet had a less steep gradient on the falling limb compared to the other monitoring locations.

The response of TP and PP closely reflected that of SSC, however TDP did not exhibit a rising limb and remained relatively constant at the inlet and outlet of the Upstream Pond (Figure 21e - 14g). TDP shows a somewhat different pattern at the outlet of the Central Pond with the concentration abruptly dropping below 10 µg P L^{-1} after 19:00pm. At the Downstream Pond outlet, TDP remained under 20 µg P L^{-1}, which was lower than both the inlet and outlet of the Upstream Pond which almost always stayed above 20 µg P L^{-1}. On the rising/receding limbs of the event, PP accounted for the majority (57-91 %) of transported P, after which TDP at the inlet and outlet of the Upstream Pond exceeded the particulate fraction.

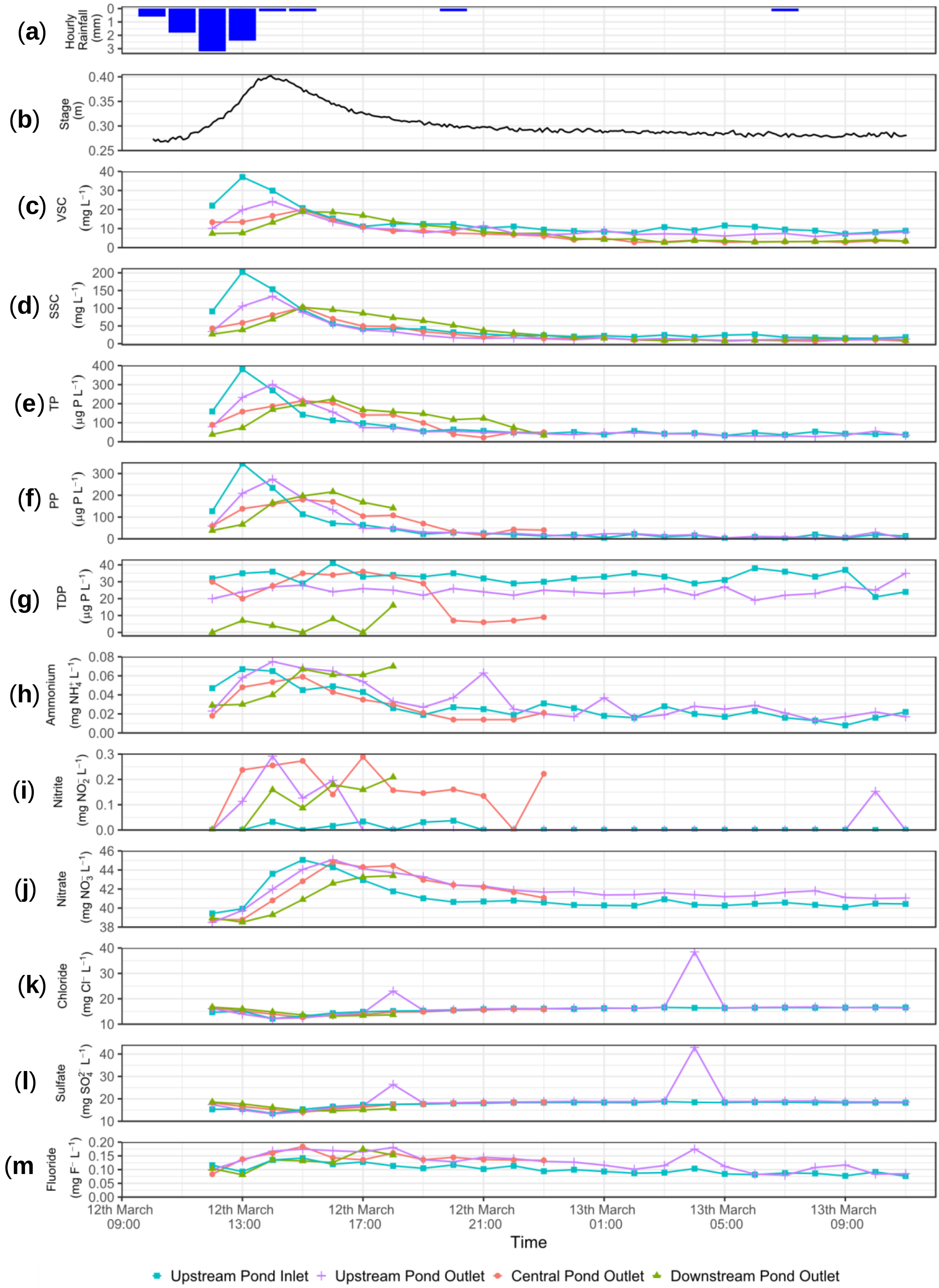

*Figure 21: Time-series during a storm event on 12th/13th March 2019 showing: (a) Hourly Rainfall (mm); (b) Stage (m) in the Central Pond; and concentrations of water quality determinands: (c) VSC and (d) SSC (mg L-1); (e) TP, (f) PP, and (g) TDP (µg P L^{-1}); (**h**) ammonium (mg NH_4^+ L^{-1}); (**i**) Nitrite (mg NO_2^- L^{-1}); (**j**) Nitrate (mg NO_3^- L^{-1}); (**k**) chloride (mg Cl^- L^{-1}); (**l**) Sulfate (mg SO_4^{2-} L^{-1}); and (**m**) Fluoride (mg F^- L^{-1}) at each pond inlet/outlet sampling site.*

On-line pond sediment quality:

From manual surveying of sediment depths approximately two years after their construction, it was estimated that 13.89 m^3 of matter had accumulated in the Upstream Pond, and 7.36 m^3 in the Central Pond. This meant that the Upstream Pond had filled ~20 % of its total capacity, and the Central ~8 %. At the time of surveying in January, depths in the Downstream Pond were unable to be measured due to the water level being too high. The Downstream Pond was able to be surveyed in July at the earliest (due to the Covid-19 pandemic), and had accumulated 9.89 m^3 of matter, equating to ~10 % of its total capacity.

Sediment traps were deployed continuously from August 2019, with sediment collection taking place on six occasions until March 2020 to capture run-off during the wet season. Throughout this 7-month period, rates of accumulation were variable, but the Upstream Pond had the highest overall accumulation, and the Downstream Pond had the lowest (Table 17). Sediment accumulation rates varied considerably between the trap placements within ponds as shown by the large standard deviations. Over the whole period, the ponds accumulated 6.1 % of the downstream catchment silt + clay flux, and 7.6 % of all suspended sediment. P accumulation in ponds generally showed the same pattern as sediment, and on average made up ~ 0.1 % of the total accumulated mass (Table 18). Total accumulated P in ponds only made up 3.2 % of the Downstream Catchment P flux. LOI showed that deposited sediments were largely made up of inorganic matter (IOM), accounting for > 75 % of the accumulated sediment mass throughout the sampling period. The OM content ranged from 10 – 23 % and consistently decreased downstream along the pond sequence in each deployment period. OM content was highest between August and October. OM content of pond sediment was significantly enriched compared to the soil in the arable fields of the contributing area which had an OM content of 5 – 7 %, typical of the arable fields in this sub-catchment.

Table 17: Accumulated sediment (±SD) (t) in each pond, all the ponds, and only the silt + clay (< 63 µm) for trap monitoring periods. Accumulated sediment yield (t ha^{-1}) for all ponds from the contributing area (30 ha), the flux of sediment and silt + clay (t) and the exported yield (t ha^{-1}) from the Downstream Catchment area (340 ha) are given for the same periods.

Monitoring Period	Days	Rainfall (mm)	Accumulated Sediment (t)					All Ponds Sediment Yield (t ha^{-1})	Catchment Sediment Flux (t)	Catchment silt+clay Flux (t)	Catchment Sediment Yield (t ha^{-1})
			Upstream Pond	Central Pond	Downstream Pond	All Ponds	All Ponds (silt+clay)				
08/08/2019 – 30/08/2019	22	62	0.56 ± 0.27	0.54 ± 0.35	0.33 ± 0.35	1.43 ± 0.56	1.01	0.048	0.34	0.3	0.001
30/08/2019 – 03/10/2019	34	128	0.63 ± 0.55	0.17 ± 0.05	0.25 ± 0.04	1.06 ± 0.55	0.71	0.035	7.4	6.47	0.022
03/10/2019 – 30/10/2019	27	132	0.69 ± 0.27	0.32 ± 0.11	-	1.01 ± 0.29	0.65	0.034	19.06	16.66	0.056
30/10/2019 – 04/12/2019	35	140	0.63 ± 0.37	0.39 ± 0.2	-	1.02 ± 0.42	0.67	0.034	21.93	19.16	0.065
04/12/2019 – 22/01/2020	49	167	0.67 ± 0.27	0.82 ± 0.28	0.67 ± 0.23	2.16 ± 0.45	1.57	0.072	32.79	28.65	0.096
22/01/2020 – 12/03/2020	50	177	0.98 ± 0.35	1.05 ± 0.33	0.49 ± 0.31	2.52 ± 0.57	1.77	0.084	38.63	33.76	0.114
Total	217	871	4.15 ± 0.89	3.29 ± 0.6	1.74 ± 0.52	9.18 ± 1.19	6.38	0.306	120.18	104.99	0.353

Table 18: Accumulated phosphorus (±SD) (kg) in each pond and all three ponds for sediment trap monitoring periods. Accumulated P yield (kg ha^{-1}) for all ponds from the contributing area (30 ha), the flux of P (kg) and the exported P yield (kg ha^{-1}) from the Downstream Catchment area (340 ha) are given for the same periods.

Monitoring Period	Days	Rainfall (mm)	Accumulated P (kg)				All Ponds P Yield (kg ha^{-1})	Catchment P Flux (kg)	Catchment P Yield (kg ha^{-1})
			Upstream Pond	Central Pond	Downstream Pond	All Ponds			
08/08/2019 – 30/08/2019	22	62	0.58 ± 0.27	0.51 ± 0.34	0.29 ± 0.28	1.38 ± 0.52	0.046	1.06	0.003
30/08/2019 – 03/10/2019	34	128	0.69 ± 0.55	0.22 ± 0.08	0.27 ± 0.04	1.18 ± 0.56	0.039	16.42	0.048
03/10/2019 – 30/10/2019	27	132	0.65 ± 0.18	0.36 ± 0.12	-	1.01 ± 0.22	0.034	43.87	0.129
30/10/2019 – 04/12/2019	35	140	0.56 ± 0.29	0.4 ± 0.19	-	0.96 ± 0.35	0.032	54.7	0.161
04/12/2019 – 22/01/2020	49	167	0.6 ± 0.22	0.81 ± 0.27	0.69 ± 0.25	2.1 ± 0.43	0.07	77.64	0.228
22/01/2020 – 12/03/2020	50	177	0.91 ± 0.22	0.94 ± 0.48	0.42 ± 0.27	2.27 ± 0.59	0.076	87.91	0.259
Total	**217**	**871**	**3.99 ± 0.77**	**3.24 ± 0.69**	**1.68 ± 0.46**	**8.91 ± 1.13**	**0.297**	**281.6**	**0.828**

4.6 Water storage in FSAs during storm events and estimated reductions in catchment outlet flows

FSA water level data have been analysed in order to assess the effectiveness of the south sub-catchment (3.4 km^2) FSAs, which have an estimated combined storage capacity of 15,717 m^3. The volume of each FSA was calculated using the methods detailed in Section 2.7. This analysis has not been done in the north sub-catchment due to absence of LiDAR or survey data for the newer FSA interventions and suspect data in one of the FSAs for much of the monitoring period (Section 3.5).

Three of the largest storm events observed in each water year from 2019/2020 to 2021/2022 have been analysed, with return periods of up to 5.5 years. These events were identified from the CM site south sub-catchment outlet discharge time-series, estimated using the methods detailed in Section 2.5 (Figure 22).

The start of each event was identified by the start of locally recorded rainfall, and the antecedent storage volume was taken at this time, as a percentage of the total storage volume available.

Each FSA volume time-series was shifted to account for the travel time to the CM site sub-catchment outlet discharge location. Travel time was calculated using the estimated mean channel velocity (Section 2.4) and the distance from FSA outlet to the CM site.

To assess the sensitivity to travel time, the analysis was repeated with ±25% and ±10% travel time shifts in each FSA volume time-series. For each travel time scenario the sum of all FSA volumes was averaged to a one-hour volumes to give a better estimate of the total sustained FSA volume, due to short-term variability in the 5-minute time-series. Hourly flood volume was calculated from the CM discharge time-series and hourly periods were centred on the flood peak to ensure representation of the flood maximum.

The percentage of total FSA stored flood volume was calculated as a proportion of the FSA volume increase added to the 1-hour flood volume, giving an estimate of the reduction in downstream discharge.

Results showed reductions in flood peaks across all events, ranging from 14.2% to 55.2% during the most intense rainfall event (Table 19). As the proportion of water stored is highest for the largest and most intense events this indicates a threshold effect, that higher stream water levels result in more overbank flow into the FSAs to be stored. This suggests that the NFM potential for flood water storage is greater in larger events, where overbank flow was observed at spillways and leaky barriers than during smaller events where FSAs fill from runoff. However, the smallest peaks analysed (15/02/2022 and 16/03/2022) were still reduced by over 20%, with over 1,300 m^3 combined water storage. The hydrographs in Figure 23, Figure 24 and Figure 25 show successful attenuation flood peaks for all events. This is demonstrated by reduced discharge due to flood water storage during the rising limb, event peak and at the start of the falling limb, after which FSA drainage increased the discharge on the falling limb.

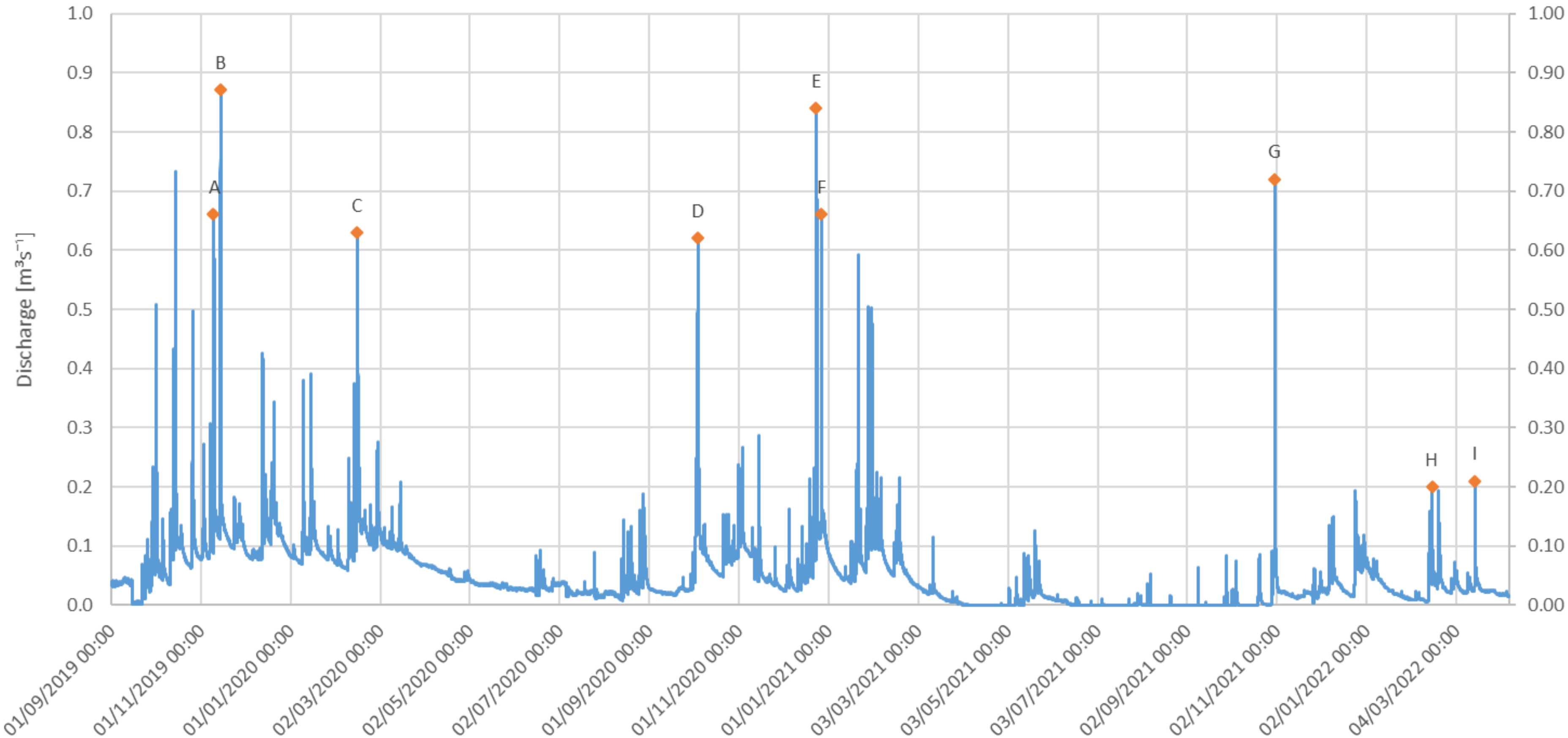

Figure 22: Time-series of discharge at the sub-catchment outlet monitoring site CM, with analysed storm events marked by orange symbols and assigned letter. Event dates - A: 09/11/2019, B: 14/11/2019, C: 15/02/2020, D: 04/10/2020, E: 23/12/2020, F: 27/12/202. Note that the October 2019 storm event was not analysed as the time-series data were not available for one of the larger FSAs during this period, so total flood storage volume could not be reliably estimated.

Table 19: Storm event summary statistics. South sub-catchment an estimated combined storage capacity of 15,717 m^3. ***Instant peak discharge*** *= Instantaneous maximum discharge (in meters cubed per second) observed during each storm event.* ***Max12 hr rainfall*** *= maximum amount of rainfall (in millimetres) observed in a consecutive 12-hour period during each event.* ***Antecedent stored volume*** *= total FSA volume at the start of the event rainfall.* ***Max stored volume*** *= the maximum volume of water stored in the FSAs (i.e. the maximum total FSA volume minus the antecedent volume).* ***Min remaining total storage*** *= the amount of remaining FSA capacity at the highest FSA volume during the event.* ***Peak total volume*** *= average total FSA volume (antecedent volume plus stored volume) over the hour period centred on the flood peak.* ***Hourly reduction in flood peak*** *= stored volume as a percentage of the total flood volume plus the change in stored volume, over the hour peak of the storm event. All volumes are shown as a percentage of total storage capacity or in cubic meters. Volumes are estimated using the mean stream travel time (estimated using the distance of each FSA to the sub-catchment outlet monitoring site and the estimated mean channel velocity from salt dilution time-of-travel experiment detailed in Section 2.4). The volume ranges in brackets show results from ±25% and ±10% mean travel time sensitivity analysis.*

Event	Event date	Instant Peak Discharge [m³s⁻¹]	Max 12 hr Rainfall [mm]	Antecedent stored volume [%]	Max stored volume [%]	Max stored volume [m³]	Min remaining total storage [%]	Min remaining total storage [m³]	Peak total volume [%]	Peak total volume [m³]	Hourly reduction in flood peak [%]
A	09/11/19	0.66	23.6	5.4 (5.4-5.4)	13.9 (13.9-14.0)	2193 (2193-2200)	80.7 (80.6-80.7)	12680 (12673-12682)	16.6 (16.0-17.1)	2602 (2519-2693)	14.2 (13.4-14.4)
B	14/11/19	0.87	29.4	7.4 (7.4-7.5)	25.4 (25.3-25.4)	3992 (3976-3992)	67.2 (67.2-67.2)	10559 (10555-10564)	26.3 (25.1-27.8)	4132 (3943-4363)	26.8 (26.3-27.0)
C	15/02/20	0.63	14.8	8.3 (8.2-8.3)	20.3 (20.2-20.3)	3190 (3174-3190)	79.7 (79.7-79.8)	12530 (12527-12538)	17.5 (17.0-18.0)	2746 (2674-2829)	18.5 (17.8-19.2)
D	04/10/20	0.62	27.8	9.7 (9.6-9.8)	16.7 (16.6-16.9)	2625 (2609-2656)	73.6 (75.6-75.6)	11564 (11564-11566)	18.0 (17.7-18.4)	2828 (2778-2885)	14.6 (14.0-14.8)
E	23/12/20 (Peak 1)	0.83	35.8	10.7 (10.7-10.7)	49.1 (49.0-49.4)	7717 (7701-7764)	40.2 (40.0-40.3)	6326 (6284-6339)	35.5 (29.8-40.6)	5577 (4690- 6382)	55.2 (49.9-57.6)
F	23/12/20 (Peak 2)	0.84							53.6 (52.4-55.3)	8430 (8230-8697)	19.1 (14.5-23.8)
G	27/12/20	0.66	19.2	13.0 (13.0-13.0)	19.8 (19.7-19.9)	3112 (3096-3128)	67.2 (67.3-67.2)	10563 (10557-10581)	26.5 (25.3-27.9)	4170 (3970-4392)	32.4 (32.1-33.1)
H	31/10/21	0.72	25.4	2.8 (2.8-2.8)	17.0 (17.0-17.0)	2672 (2672-2672)	80.2 (80.1-80.2)	12598 (12596-12606)	18.0 (17.0-18.9)	2830 (2679-2964)	31.8 (28.6-33.2)
I	15/02/22	0.20	10.2	4.6 (4.6-4.7)	4.1 (4.0-4.1)	644 (629-644)	91.3 (91.3-91.3)	14354 (14353-14355)	6.3 (6.1-6.7)	994 (952-1047)	20.1 (15.9-18.4)
J	16/03/22	0.21	17.6	3.4 (3.4-3.4)	5.3 (5.3-5.3)	833 (833-833)	91.3 (91.3-9.13)	14352 (14351-14353)	5.9 (5.6-6.3)	931 (887-987)	21.7 (19.8-23.6)

The maximum flood reduction of 55.2% was observed during the 23 December 2020 event which had two peaks, the longest duration and most intense rainfall. The daily rainfall and API were both highest for this event (Section 4.1), showing that the FSA interventions were effective during notably wet preceding conditions. As significant storage capacity remained after the first peak the FSAs were also able to attenuate a second larger peak by 19.1%, during which the FSAs held over 8,000 m^3 of water. While both peaks were successfully attenuated, drainage of the FSAs after the first peak and resultant increase in discharge at the sub-catchment outlet will have reduced the effect for the second peak. This event also showed the largest sensitivity to travel time, with an estimated 9.3% increase in flood peak reduction between +25% travel time and -25% travel time. Suggesting that slower travel times and drainage would attenuate the peak further. This relationship was observed across all events.

At least 40% of total storage capacity remained available throughout all events, suggesting that larger events than those analysed here could be successfully attenuated. Though this will be dependent on how much flood storage capacity is lost to antecedent conditions. The maximum antecedent storage observed was 13% during notably wet 2020 winter event on 27 December 2020 which closely succeeded the longest and most intense event observed, yet over 67% of storage capacity remained throughout the event. There is a wide range of responses to storm events dependent on antecedent conditions and rate and duration of rainfall. Further work is being carried out to investigate these relationships through a PhD studentship.

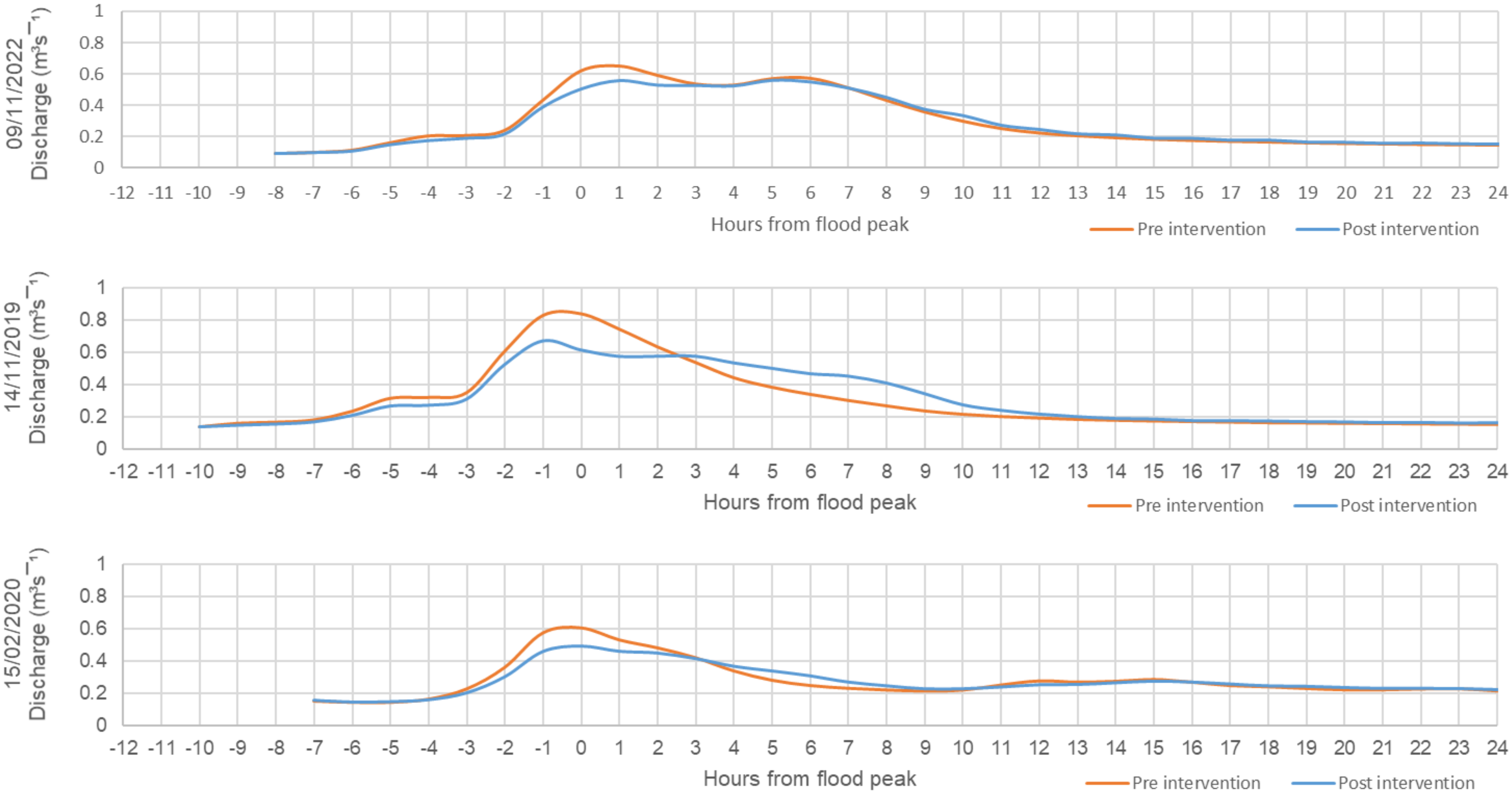

Figure 23: WY 2019/2020 event hydrographs for discharge pre- (orange) and post- FSA interventions (blue). The post intervention discharge is the hourly averaged value estimated at the sub-catchment outlet using the stage-discharge rating curve and repeat observations of water level. The pre intervention discharge is estimated from the post intervention discharge by subtracting the post intervention discharge multiplied by the stored FSA volume as a percentage of the combined stored and flood volume at the sub-catchment outlet.

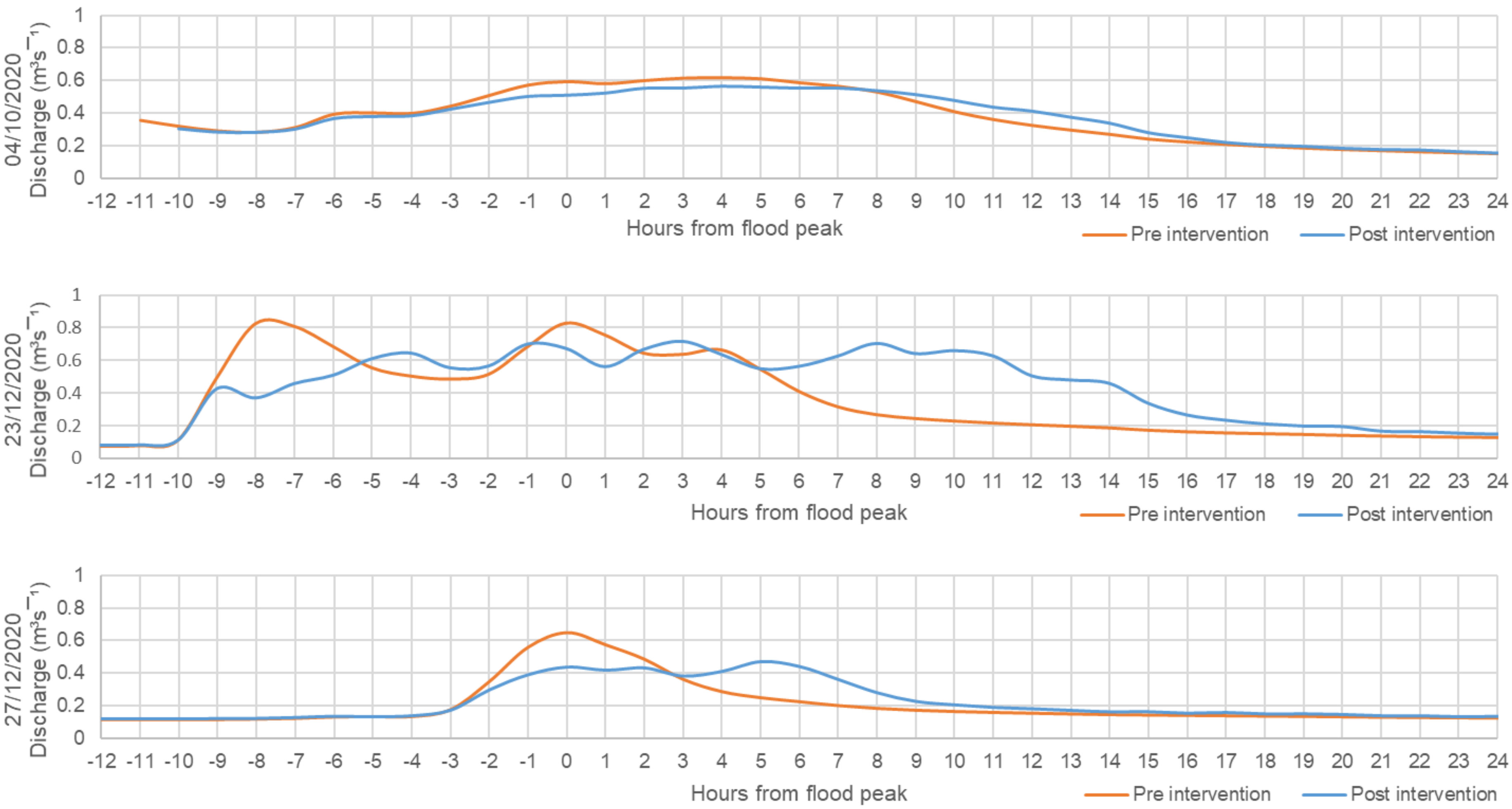

Figure 24: WY 2020/2021 event hydrographs for discharge pre- (orange) and post- FSA interventions (blue). The post intervention discharge is the hourly averaged value estimated at the sub-catchment outlet using the stage-discharge rating curve and repeat observations of water level. The pre intervention discharge is estimated from the post intervention discharge by subtracting the post intervention discharge multiplied by the stored FSA volume as a percentage of the combined stored and flood volume at the sub-catchment outlet.

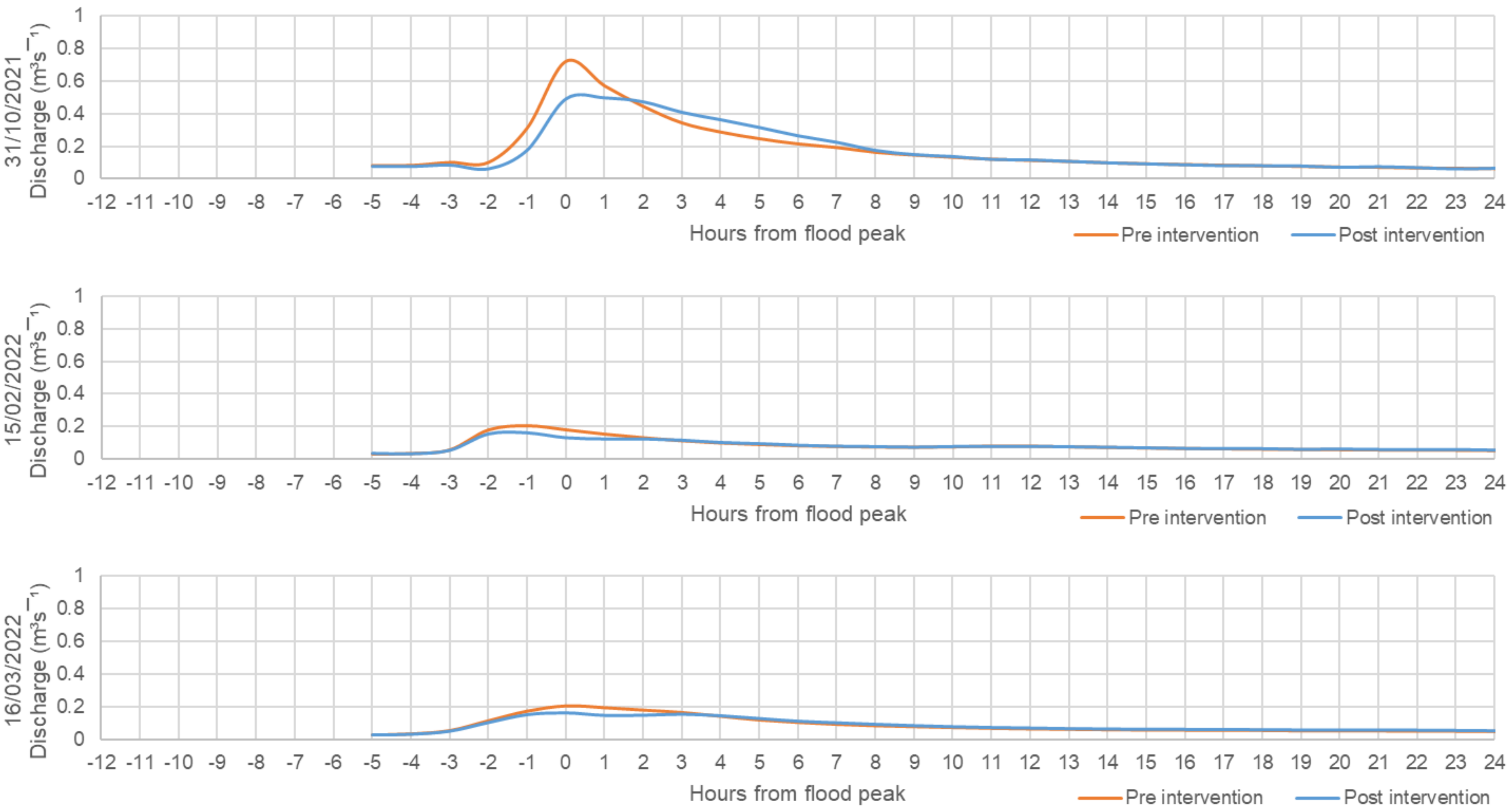

Figure 25: WY 2021/2022 event hydrographs for discharge pre- (orange) and post- FSA interventions (blue). The post intervention discharge is the hourly averaged value estimated at the sub-catchment outlet using the stage-discharge rating curve and repeat observations of water level. The pre intervention discharge is estimated from the post intervention discharge by subtracting the post intervention discharge multiplied by the stored FSA volume as a percentage of the combined stored and flood volume at the sub-catchment outlet.

5 Monitoring Evaluation

Data were evaluated using a number of approaches at multiple spatial scales in order to determine the effect of the NFM interventions.

Isolating the effect of NFM interventions from natural variability was challenging using an experimental ‘Before-After Control-Impact’ (BACI) approach, particularly as the catchment interventions were incrementally added throughout the monitored period (Robotham, 2022). This approach requires robust pre-intervention data to eliminate the noise of environmental and climatic change within catchments, relative to the effects of NFM interventions. This trial was characterised by a relatively short and dry pre-intervention period, with few high magnitude storm events. This was followed by a wet post-intervention period, making it difficult to compare pre- and post-NFM data to detect the effects. For a better assessment of NFM effectiveness we recommend a prolonged period of multi-scale baseline monitoring that captures a range of environmental conditions pre-intervention installation, to allow for more robust before-after evaluation.

Combining in-stream and individual intervention-scale monitoring provided us with evidence of the FSA NFM intervention effectiveness during storm events. Continuous water level monitoring in FSAs allowed us to calculate continuous flood storage volume across the whole south sub-catchment, enabling us to estimate the reduction in flood peaks at the downstream flood receptor rather than qualify. Further work is required to evaluate the FSA effectiveness and responses during storm events, with diverse antecedent conditions and rates and durations of rainfall. Analyses will also be carried out in the north sub-catchment when topographic data are available for all FSAs.

6 Concluding Remarks

This was a successful monitoring program with over 90% data coverage of rainfall, stream flow, FSA level, suspended sediment and associated nutrients across 5 years and two sub-catchments of the Littlestock Brook NFM scheme. These data enabled the calibration and validation of hydrodynamic modelling of the NFM measures, as well as detailed analysis of the catchment area hydrological processes and water quality. This enabled assessment of the effectiveness of the NFM interventions, within the limits of the range of conditions observed during the monitoring period.

The analysis of the intervention-scale monitoring data showed successful attenuation of all storm event discharge peaks (14.2-55.2% reductions) and that over 40% of the total storage volume remained available throughout all events. The greatest peak reductions were observed in the larger and more intense rainfall events, where higher water levels lead to greater overbank flow to the FSAs. This was the case for the largest reduction (55.2%) in flood peak for the intense rainfall 23 December 2020 event. This event was preceded by notably wet conditions and the FSA storage successfully attenuated a second storm peak by 19.1%. Travel time sensitivity analysis showed that slower travel time from FSAs to the sub-catchment outlet would attenuate flood peaks further across the events analysed. The effects varied greatly due to event variability of antecedent conditions and rainfall intensity and duration.

The FSAs were able to provide multiple benefits through significant sediment trapping, particularly during the larger storm events where features were connected to the stream via spillways. The equivalent of 15% of sub-catchment sediment yield was trapped by features over the 2-3 years since construction. This stored sediment also accounted for 10% of the TP and 8% of the POC yields. The measured sediment accumulation rates varied greatly between features, and they do not appear to compromise the primary water storage function of the FSAs; they are only likely to need maintenance every 10 years. The accumulated sediment is generally fine and enriched in nutrients thereby holding potential value for re-use in agriculture.

Detailed monitoring of the on-line pond features highlighted their benefits for water quality during baseflow conditions, significantly reducing dissolved nutrient (N and P) concentrations by 5 and 29% respectively. Overall these small features acted as a net sink of sediment, despite some instances of sediment resuspension/flushing during the monitoring period. They developed into vegetated wetland habitat, however they also accumulated sediment rapidly and therefore require maintenance approximately every 2 years.

Streamflow monitoring in each of the sub-catchments highlighted significant differences in hydrological regimes, with the south sub-catchment having higher baseflows and lower peak discharges during storm events. The north sub-catchment had a more hydrologically flashy response with higher peaks, suggesting that the NFM features located within this area will be particularly important for intercepting rapid run-off from this land.

All data collected throughout this monitoring will now be archived and made available on the NERC Environmental Information Data Centre for further research. Further analysis of these data is also being carried out through an ongoing PhD studentship, which will analyse the effectiveness of the scheme in more detail over the range of events and conditions observed.

7 Acknowledgements

This research was funded by the SCENARIO Natural Environment Research Council DTP (grant NE/L002566/1) and SPITFIRE NERC DTP (grant NE/L002531/1), with additional PhD CASE studentship funding provided by Wild Oxfordshire and Thames Water. We would also like to acknowledge the contributions of all the organisations involved in the delivery of this NFM project, notably Jo Old and David McKnight (Environment Agency), Ann Berkeley, Anne Miller and Hilary Phillips (Wild Oxfordshire), Richard Bennett and Laurence King (West Oxfordshire District Council), and David Gasca-Tucker (ECP); the time, patience and enthusiasm of the landowners and local community (Milton Parish Council and Bruern Estate) notably Chris Trotman, Jill and John Fox, David and Henry Astor and Matt Childs; the support of the Environment Agency and Hydraulics Research Wallingford in the monitoring and modelling programmes; and the Thames Regional Flood and Coastal Committee and Thames Water for their financial support alongside that of the Environment Agencies Grant in Aid programmes.

8 References

Bhatti, J. S. and Bauer, I. E. (2002) 'Comparing loss-on-ignition with dry combustion as a method for determining carbon content in upland and lowland forest ecosystems', Communications in Soil Science and Plant Analysis, 33(15–18), pp. 3419–3430. doi: 10.1081/CSS-120014535.

Bowes, M.J., Armstrong, L.K., Harman, S.A., Wickham, H.D., Nicholls, D.J.E., Scarlett, P.M., Roberts, C., Jarvie, H.P., Old, G.H., Gozzard, E., Bachiller-Jareno, N., Read, D.S., 2018. Weekly water quality monitoring data for the River Thames (UK) and its major tributaries (2009-2013): The Thames Initiative research platform. Earth Syst. Sci. Data 10, 1637–1653. https://doi.org/10.5194/essd-10-1637-2018

De Vos, B. *et al.* (2005) 'Capability of loss-on-ignition as a predictor of total organic carbon in non-calcareous forest soils', *Communications in Soil Science and Plant Analysis*, 36(19–20), pp. 2899–2921. doi: 10.1080/00103620500306080.

Dalgaard P. 2004. [R] confidence interval for nls. https://stat.ethz.ch/ [online] Available from: https://stat.ethz.ch/pipermail/r-help/2004-October/058779.html

Eisenreich, S. J., Bannerman, R. T. and Armstrong, D. E. (1975) 'A simplified phosphorus analysis technique', *Environmental Letters*, 9(1), pp. 43–53. doi: 10.1080/00139307509437455.

Herschy, R.,1993. The velocity-area method, Flow Meas. Instrum, 4, pp. 7–10

Hongve, D.,1987. A revised procedure for discharge measurement by means of the salt dilution method, Hydrological Processes, 1(3), pp. 267–270. doi: 10.1002/hyp.3360010305.

Met Office, 2006. MIDAS UK Hourly Rainfall Data.

Old, J., McKnight, D., Bennett, R., Grzybek, R., 2019. A catchment partnership approach to delivering natural flood management in the Evenlode, UK. Proc. Inst. Civ. Eng. - Eng. Sustain. 1–8. https://doi.org/10.1680/jensu.17.00038

Robotham, J., Old, G., Rameshwaran, P., Sear, D., Gasca-Tucker, D., Bishop, J., Old, J., McKnight, D., 2021. Sediment and Nutrient Retention in Ponds on an Agricultural Stream: Evaluating Effectiveness for Diffuse Pollution Mitigation. Water 13, 1640. https://doi.org/10.3390/w13121640

Robotham, J., Old, G., Rameshwaran, P., Sear, D., Trill, E., Bishop, J., Gasca-Tucker, D., Old, J., McKnight, D., 2022a. Nature-based Solutions enhance sediment and nutrient storage in an agricultural lowland catchment. Manuscript under review.

Robotham, J., Old, G., Rameshwaran, P., Trill, E., Bishop, J., 2022b. High-resolution time-series of turbidity, suspended sediment concentration, total phosphorus concentration, and discharge in the Littlestock Brook, England, 2017-2021. NERC EDS Environ. Inf. Data Cent.

Rollett, A. *et al.* (2020) *2018-19 Soil Policy Evidence Programme: Review of best practice for SOC monitoring*. Available at: https://gov.wales/sites/default/files/publications/2020-11/review-best-practice-soil-organic-carbon-monitoring.pdf.

9 Appendices

9.1 Appendix 1 – Rating curves

<u>The Heath:</u>

Low Flow Rating (used where Stage < 0.132 m):

$$Q\ [L\ s^{-1}] = 710377415.9571 \times (Stage\ [m] + 0.01)^{8.277}$$

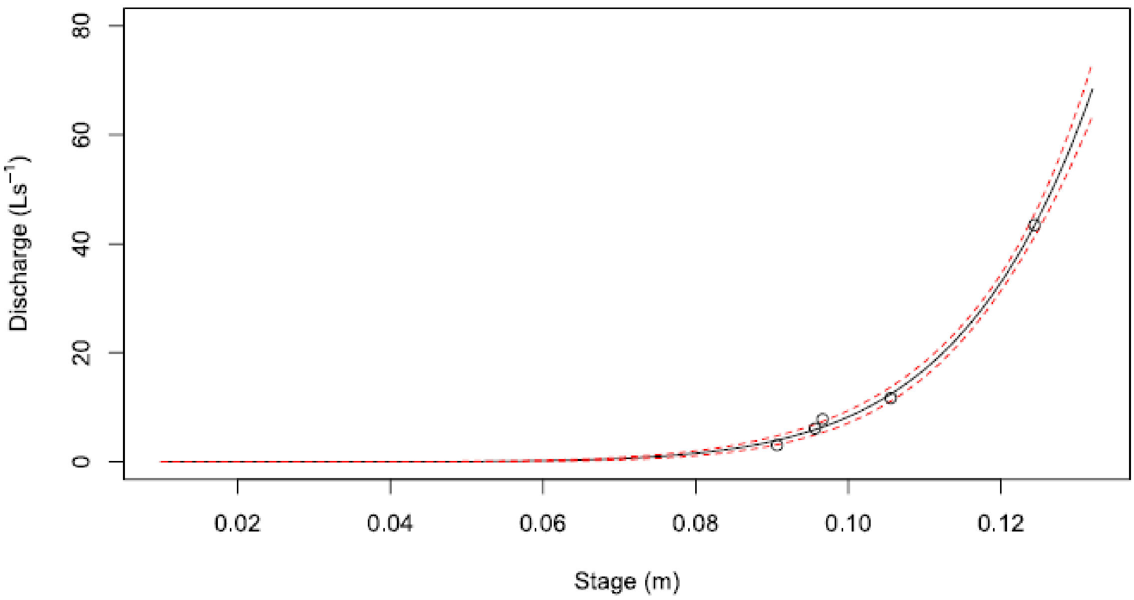

High Flow Rating (used where Stage > 0.132 m):

$$Q\ [L\ s^{-1}] = 6849.014 \times (Stage\ [m] + 0.01)^{2.3622}$$

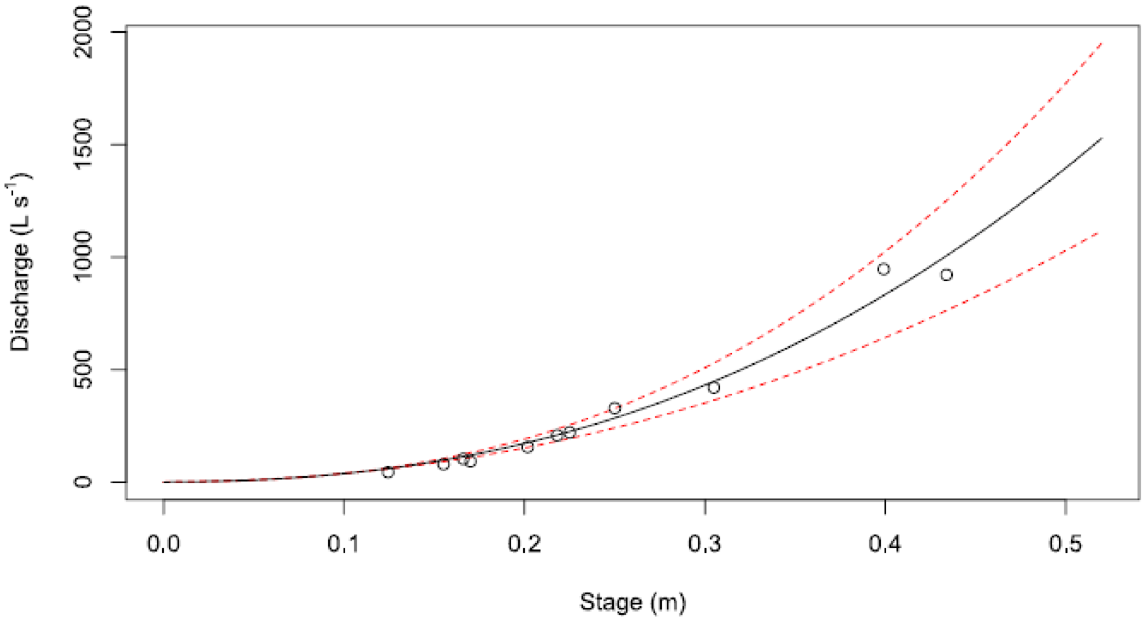

Upstream The Heath:

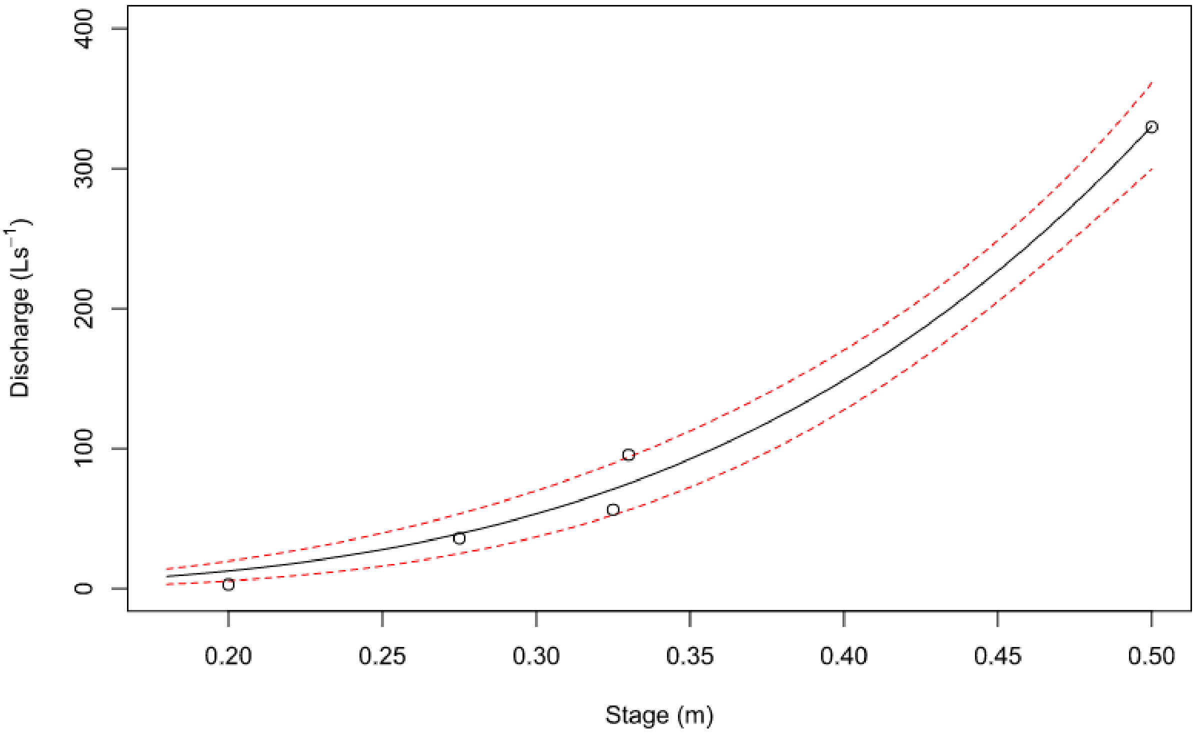

Church Meadow:

$$Q\ [L\ s^{-1}] = 1417.2706 \times (Stage\ [m] - 0.013)^{1.1669}$$

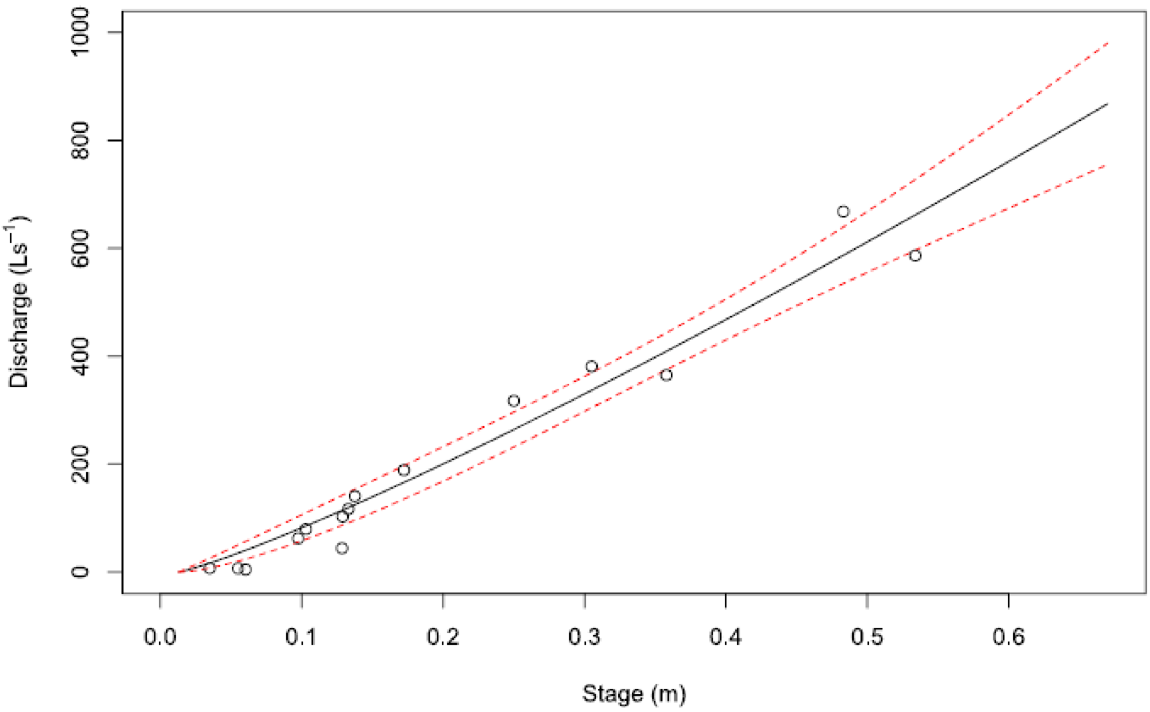

BANGOR
UK Centre for Ecology & Hydrology
Environment Centre Wales
Deiniol Road
Bangor
Gwynedd
LL57 2UW
United Kingdom
T: +44 (0)1248 374500
F: +44 (0)1248 362133

EDINBURGH
UK Centre for Ecology & Hydrology
Bush Estate
Penicuik
Midlothian
EH26 0QB
United Kingdom
T: +44 (0)131 4454343
F: +44 (0)131 4453943

LANCASTER
UK Centre for Ecology & Hydrology
Lancaster Environment Centre
Library Avenue
Bailrigg
Lancaster
LA1 4AP
United Kingdom
T: +44 (0)1524 595800
F: +44 (0)1524 61536

WALLINGFORD (Headquarters)
UK Centre for Ecology & Hydrology
Maclean Building
Benson Lane
Crowmarsh Gifford
Wallingford
Oxfordshire
OX10 8BB
United Kingdom
T: +44 (0)1491 838800
F: +44 (0)1491 692424

enquiries@ceh.ac.uk

www.ceh.ac.uk